CHAPTER 4

Chopper-Controlled DC Motor Drive

4.1 INTRODUCTION

In the case of single stage ac to dc power conversion phase-controlled converters described in Chapter 3 are used to drive the dc machines. Whenever the source is a constant-voltage dc, such as a battery or diode-bridge rectified ac supply, a different type of converter is required to convert the fixed voltage into a variable-voltage/variable-current source for the speed control of the dc motor drive. The variable dc voltage is controlled by chopping the input voltage by varying the on- and off-times of a converter, and the type of converter capable of such a function is known as a chopper.

The principle of operation of a four-quadrant chopper is explained in this chapter. The steady-state and dynamic analysis of the chopper-controlled dc motor drive and its performance characteristics are derived and evaluated. Some illustrative examples are included.

4.2 PRINCIPLE OF OPERATION OF THE CHOPPER

A schematic diagram of the chopper is shown in Figure 4.1. The control voltage to it's gate is v_c. The chopper is on for a time t_{on}, and its off time is t_{off}. Its frequency of operation is

$$f_c = \frac{1}{(t_{on} + t_{off})} = \frac{1}{T} \tag{4.1}$$

and its duty cycle is defined as

$$d = \frac{t_{on}}{T} \tag{4.2}$$

The output voltage across the load during the on-time of the switch is equal to the difference between the source voltage V_s and the voltage drop across the power

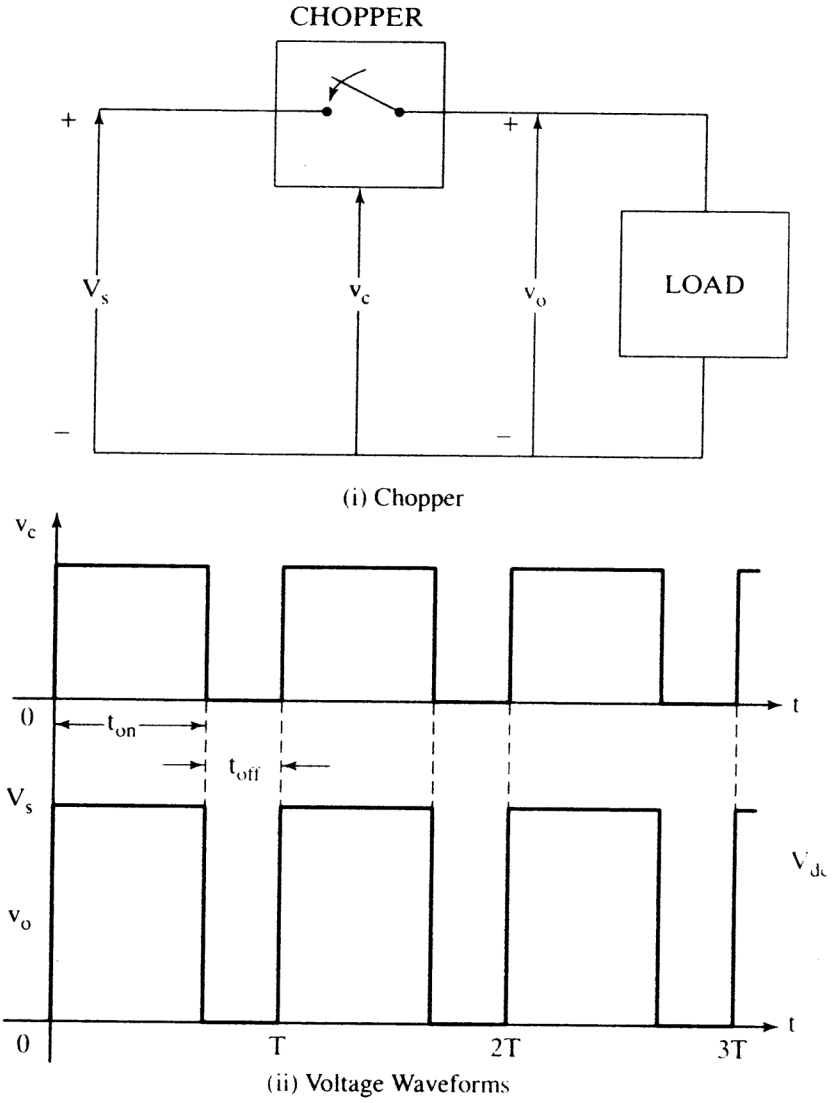

Figure 4.1 Chopper schematic and its waveforms

switch. Assuming that the switch is ideal, with zero voltage drop, the average output voltage V_{dc} is given as

$$V_{dc} = \frac{t_{on}}{T} V_s = dV_s \tag{4.3}$$

where V_s is the source voltage.

Varying the duty cycle changes the output voltage. Note that the output voltage follows the control voltage, as shown in Figure 4.1, signifying that the chopper is a voltage amplifier. The duty cycle d can be changed in two ways:

(i) By keeping the switching/chopping frequency constant and varying the on-time, to get a changing duty cycle.

(ii) Keeping the on-time constant and varying the chopping frequency, to obtain various values of the duty cycle.

A constant switching frequency has the advantages of predetermined switching losses of the chopper, enabling optimal design of the cooling for the power circuit, and predetermined harmonic contents, leading to an optimal input filter. Both of these advantages are lost by varying the switching frequency of the chopper; hence, this technique for chopper control is not prevalent in practice.

4.3 FOUR-QUADRANT CHOPPER CIRCUIT

A four-quadrant chopper with transistor switches is shown in Figure 4.2. Each transistor has a freewheeling diode across it and a snubber circuit to limit the rate of rise of the voltage. The snubber circuit is not shown in the figure.

The load consists of a resistance, an inductance, and an induced emf. The source is dc, and a capacitor is connected across it to maintain a constant voltage. The base drive circuits of the transistors are isolated, and they reproduce and amplify the control signals at the output. For the sake of simplicity, it is assumed that the switches are ideal and hence, the base drive signals can be used to draw the load voltage.

4.3.1 First-Quadrant Operation

First-quadrant operation corresponds to a positive output voltage and current. This is obtained by triggering T_1 and T_2 together, as is shown in Figure 4.3; then the load voltage is equal to the source voltage. To obtain zero load voltage, either T_1 or T_2 can be turned off. Assume that T_1 is turned off; then the current will decrease in the power switch and inductance. As the current tries to decrease in the inductance, it will have a voltage induced across it in proportion to the rate of fall of current with a polarity opposite to the load-induced emf, thus forward-biasing diode D_4. D_4 provides the path for armature current continuity during this time. Because of this, the circuit configuration changes as shown in Figure 4.4. The load is short-circuited, reducing its voltage to zero. The current and voltage waveforms for continuous and

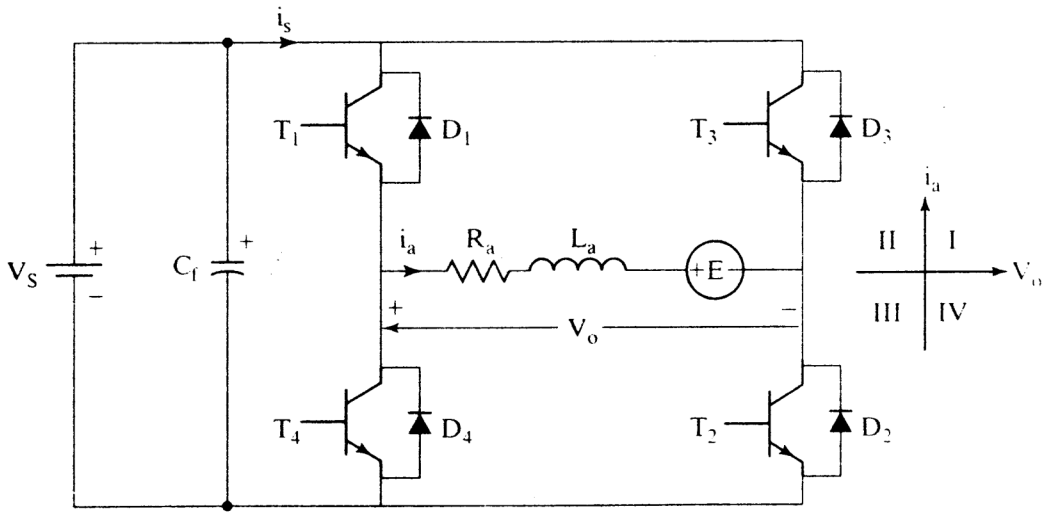

Figure 4.2 A four-quadrant chopper circuit

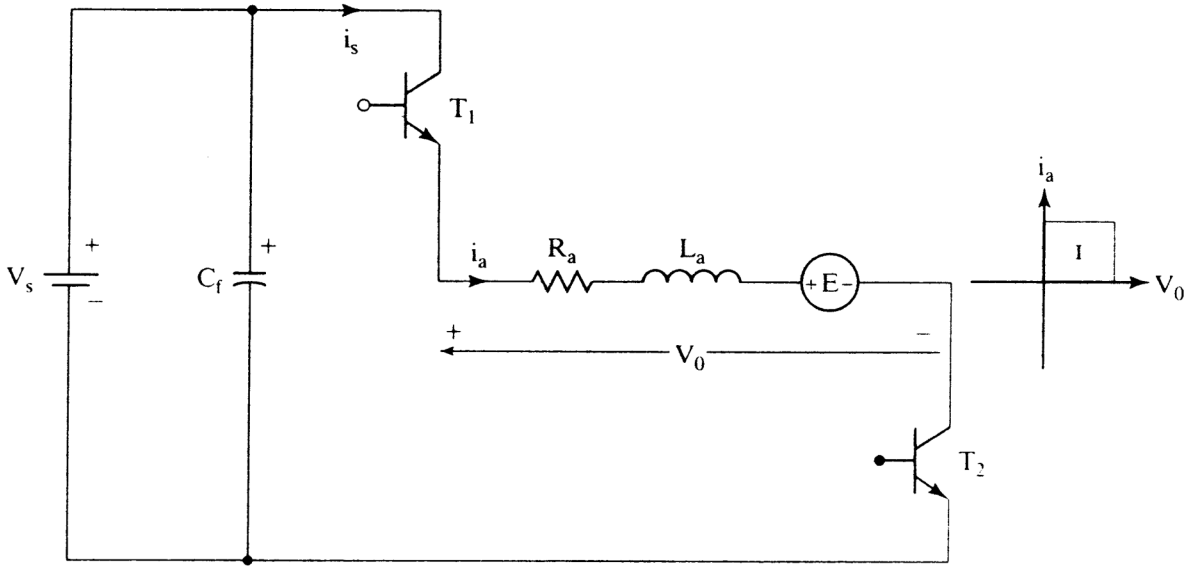

Figure 4.3 First-quadrant operation with positive voltage and current in the load

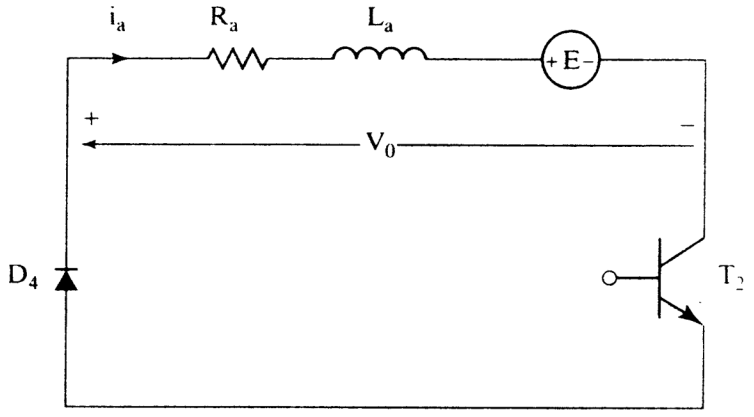

Figure 4.4 First-quadrant operation with zero voltage across the load

discontinuous current conduction are shown in Figure 4.5. Note that, in the discontinuous current-conduction mode, the induced emf of the load appears across the load when the current is zero. The load voltage, therefore, is a stepped waveform. The operation discussed here corresponds to motoring in the clockwise direction, or *forward motoring.* It can be observed that the average output voltage will vary from 0 to V_s; the duty cycle can be varied only from 0 to 1.

The output voltage can also be varied by another switching strategy. Armature current is assumed continuous. Instead of providing zero voltage during turn-off time to the load, consider that T1 and T2 are simultaneously turned off, to enable conduction by diodes D3 and D4. The voltage applied across the load then is equal to the negative source voltage, resulting in a reduction of the average output voltage. The disadvantages of this switching strategy are as follows:

(i) Switching losses double, because two power devices are turned off instead of one only.

(ii) The rate of change of voltage across the load is twice that of the other strategy. If the load is a dc machine, then it has the deleterious effect of causing

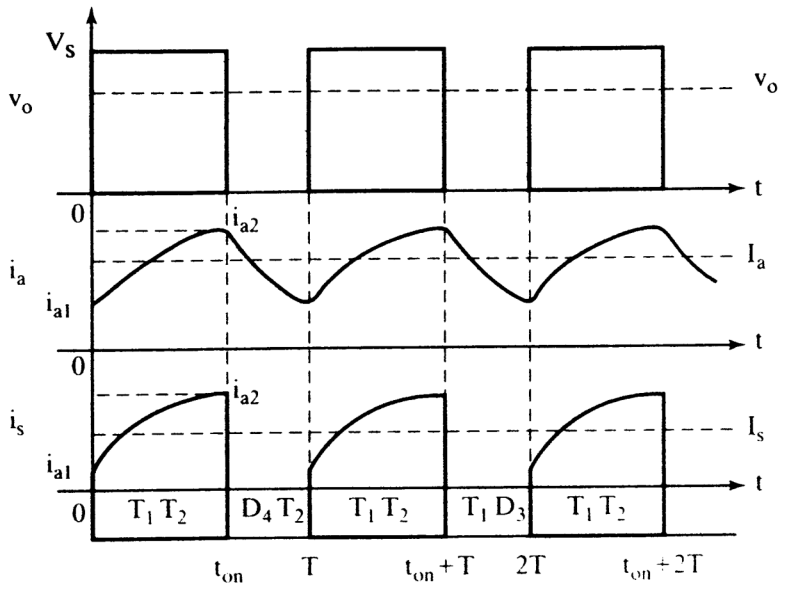

(i) Continuous Conduction

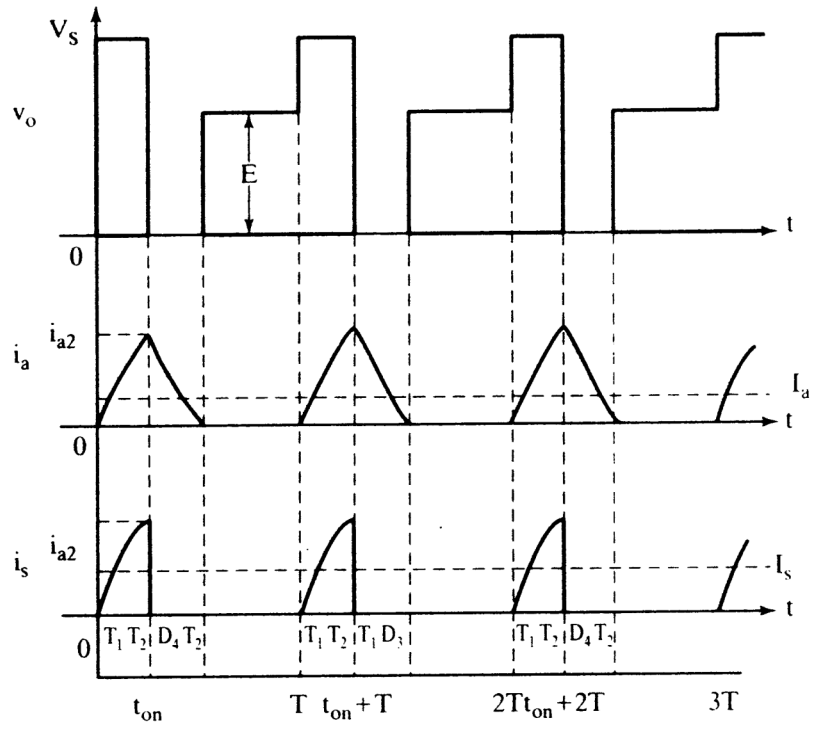

(ii) Discontinuous Conduction

Figure 4.5 Voltage and current waveforms in first-quadrant operation

higher dielectric losses in the insulation and therefore reduced life. Note that the dielectric is a capacitor with a resistor in series.

(iii) The rate of change of load current is high, contributing to vibration of the armature in the case of the dc machine.

(iv) Since a part of the energy is being circulated between the load and source in every switching cycle, the switching harmonic current is high, resulting in additional losses in the load and in the cables connecting the source and converter.

Therefore, this switching strategy is not considered any further in this chapter.

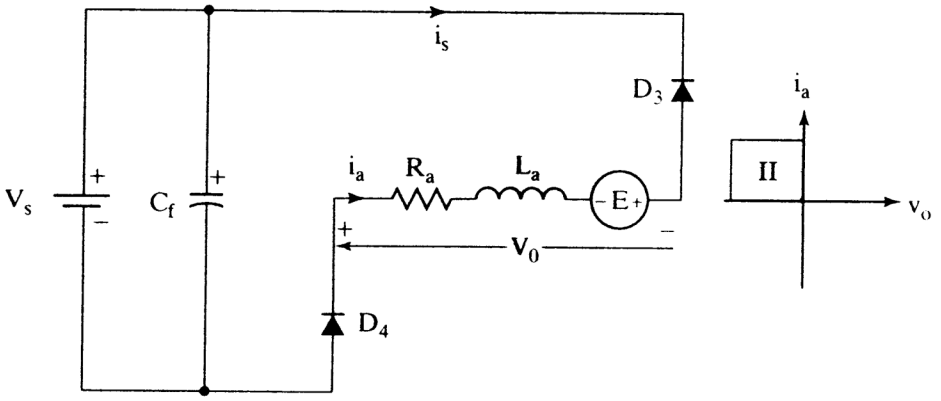

Figure 4.6 Second-quadrant operation, with negative load voltage and positive current

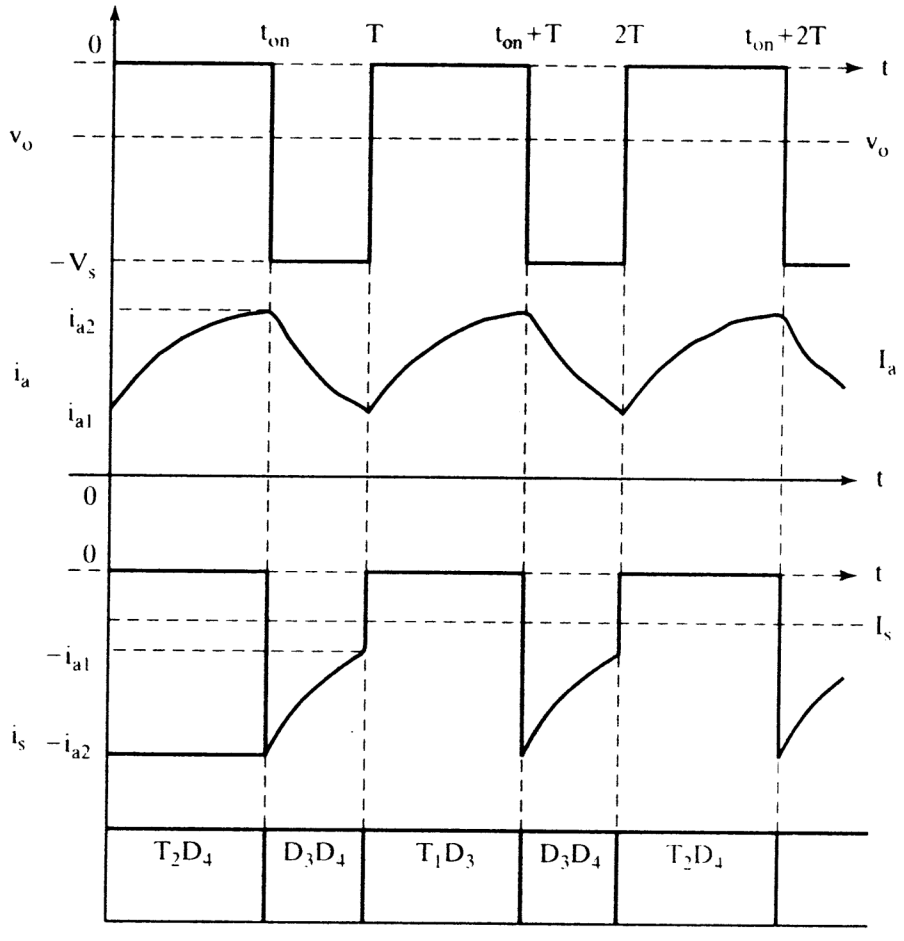

Figure 4.7 Second-quadrant operation of the chopper

4.3.2 Second-Quadrant Operation

Second-quadrant operation corresponds to a positive current with a negative voltage across the load terminals. Assume that the load's emf is negative. Consider that T_1 or T_2 is conducting at a given time. The conducting transistor is turned off. The current in the inductive load has to continue to flow until the energy in it is depleted to zero. Hence, the diodes D_3 and D_4 will take over, maintaining the load current in the same direction, but the load voltage is negative in the new circuit configuration, as is shown in Figure 4.6. The voltage and current waveforms are shown in Figure 4.7. When diodes D_3 and D_4 are conducting, the source receives power from the load. If the

source cannot absorb this power, provision has to be made to consume the power. In that case, the overcharge on the filter capacitor is periodically dumped into a resistor connected across the source by controlling the on-time of a transistor in series with a resistor. This form of recovering energy from the load is known as regenerative braking and is common in low-HP motor drives, where the saving in energy might not be considerable or cost-effective. When the current in the load is decreasing, T_2 is turned on. This allows the short-circuiting of the load through T_2 and D_4, resulting in an increase in the load current. Turning off T_2 results in a pulse of current flowing into the source via D_3 and D_4. This operation allows the priming up of the current and a building up of the energy in the inductor from the load's emf, thus enabling the transfer of energy from the load to the source. Note that it is possible to transfer energy from load to source even when E is lower in magnitude than V_s. This particular operational feature is sometimes referred to as *boost operation* in dc-to-dc power supplies. Priming up the load current can also be achieved alternatively, by using T_1 instead of T_2.

4.3.3 Third-Quadrant Operation

Third-quadrant operation provides the load with negative current and voltage. A negative emf source, $-E$, is assumed in the load. Switching on T_3 and T_4 increases the current in the load, and turning off one of the transistors short-circuits the load, decreasing the load current. That way, the load current can be controlled within the externally set limits. The circuit configurations for the switching instants are shown in Figure 4.8. The voltage and current waveforms under continuous and discontinuous

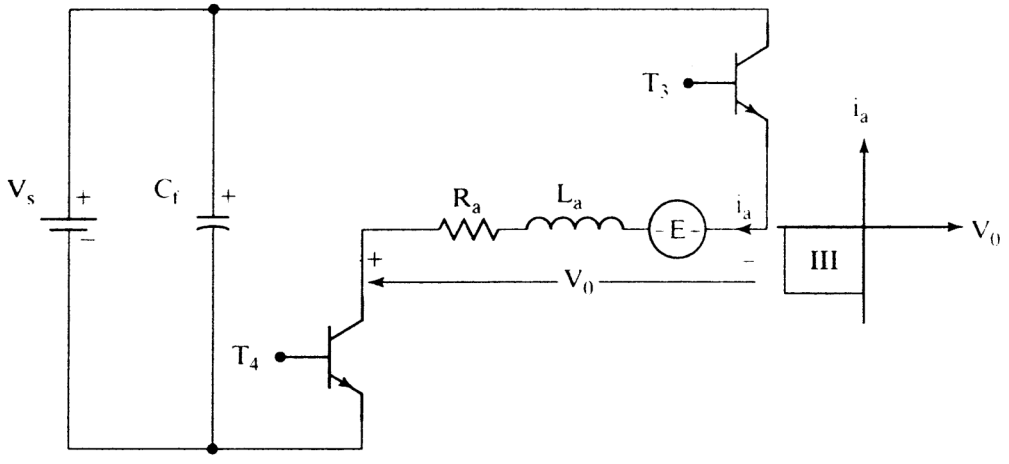

(i) Increasing load current

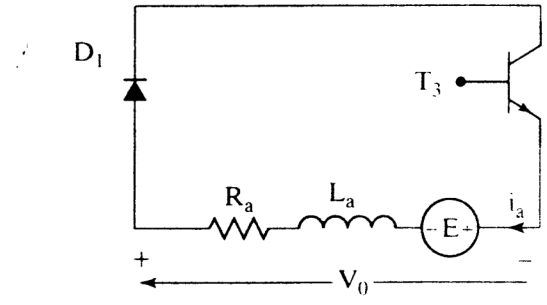

(ii) Decreasing load current

Figure 4.8 Modes of operation in the third quadrant

current-conduction modes are shown in Figure 4.9. Note the similarity between first- and third-quadrant operation.

4.3.4 Fourth-Quadrant Operation

Fourth-quadrant operation corresponds to a positive voltage and a negative current in the load. A positive load-emf source E is assumed. To send energy to the dc source from the load, note that the armature current has to be established to flow

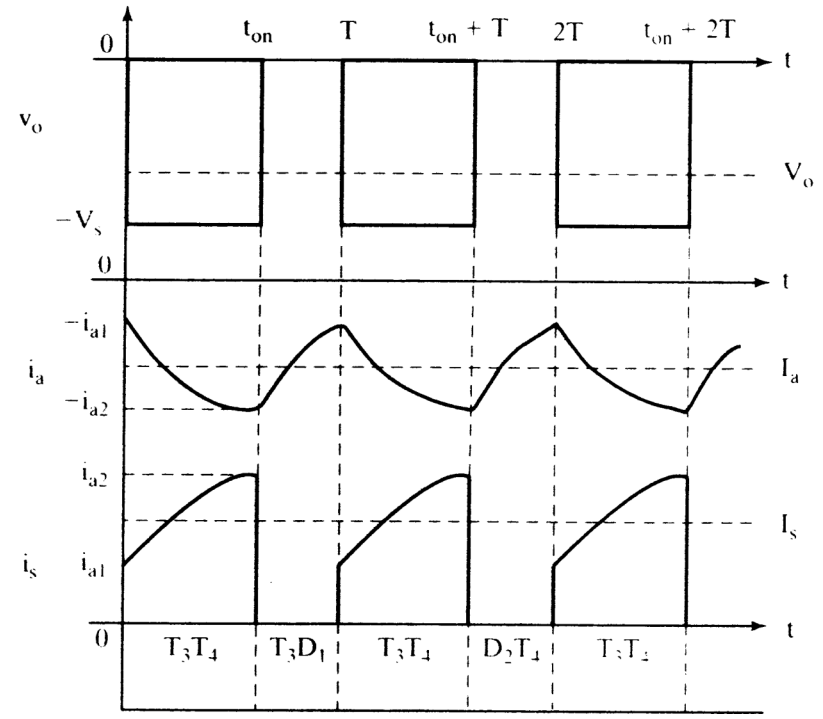

(i) Continuous Conduction

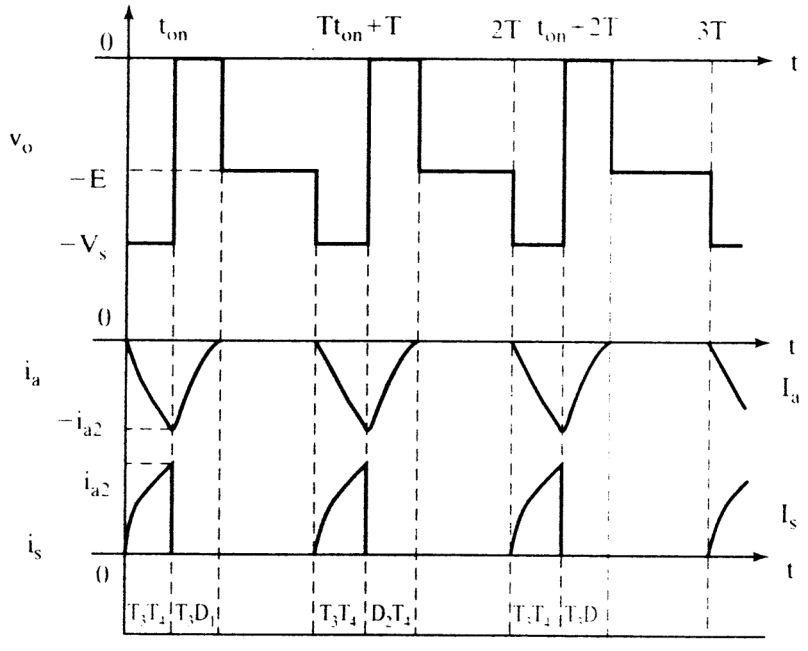

(ii) Discontinuous Conduction

Figure 4.9 Third-quadrant operation

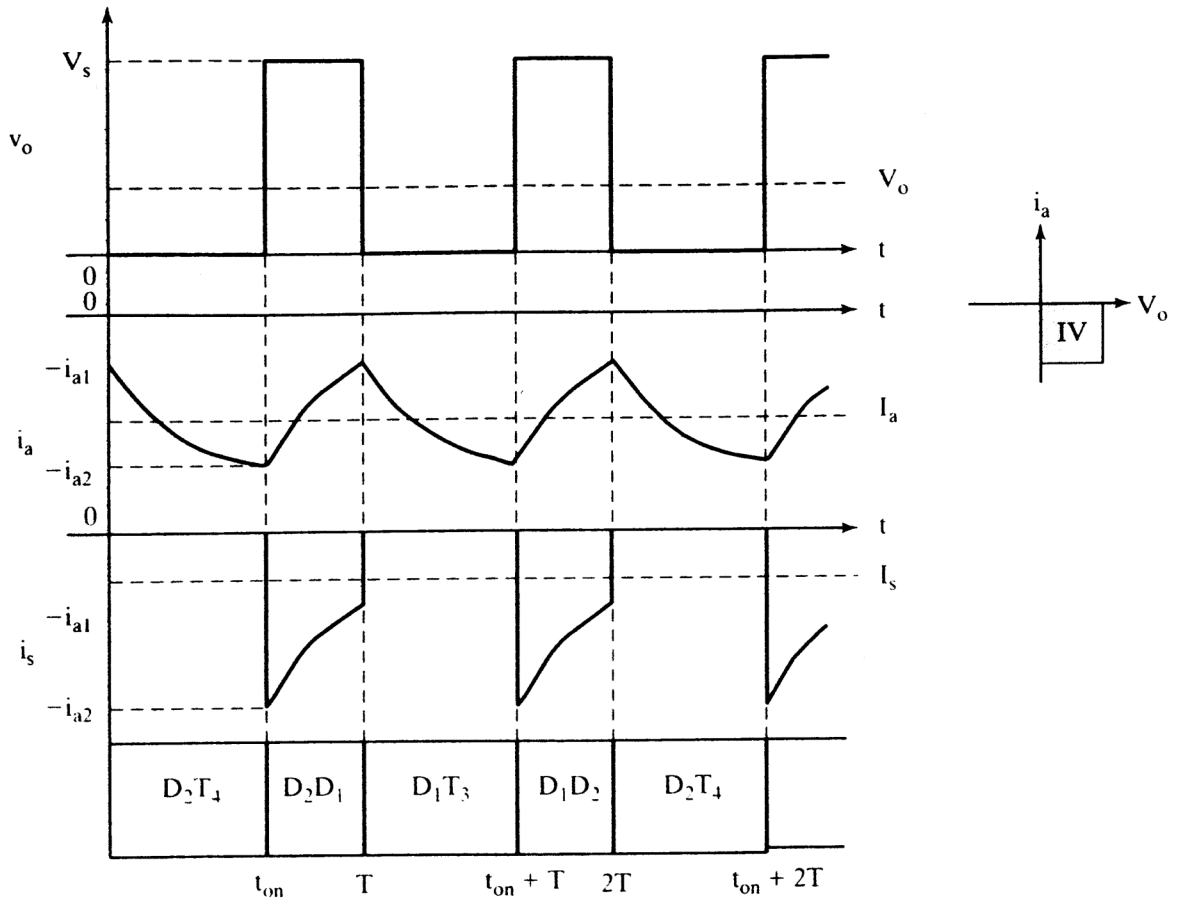

Figure 4.10 Fourth-quadrant operation of the chopper

from the right side to the left side as seen in Figure 4.2. By the convention adopted in this book, that direction of current is negative. Assume that the machine has been operating in quadrant I with a positive current in the armature. When a brake command is received, the torque and armature current command goes negative. The armature current can be driven negative from its positive value through zero. Opening T_1 and T_2 will enable D_3 and D_4 to allow current via the source, reducing the current magnitude rapidly to zero. To establish a negative current, T_4 is turned on. That will short-circuit the load, making the emf source build a current through T_4 and D_2. When the current has reached a desired peak, T_4 is turned off. That forces D_1 to become forward-biased and to carry the load current to the dc input source via D_2 and the load. When the current falls below a lower limit, T_4 is again turned on, to build up the current for subsequent transfer to the source. The voltage and current waveforms are shown in Figure 4.10. The average voltage across the load is positive, and the average load current is negative, indicating that power is transferred from the load to the source. The source power is the product of average source current and average source voltage, and it is negative, as is shown in Figure 4.10.

4.4 CHOPPER FOR INVERSION

The chopper can be viewed as a single-phase inverter because of its ability to work in all the four quadrants, handling leading or lagging reactive loads in series with an emf source. The output fundamental frequency is determined by the rate at which

the forward-to-reverse operation is performed in the chopper. The chopper is the building block for a multiphase inverter.

4.5 CHOPPER WITH OTHER POWER DEVICES

Choppers are realized with MOSFETs, IGBTs, GTOs, or SCRs, depending upon the power level required. The MOSFET and transistor choppers are used at power levels up to 50 kW. Beyond that, IGBTs, GTOs, and SCRs are used for the power switches. Excepting SCR choppers, all choppers are self-commutating and hence have a minimum number of power switches and auxiliary components. In the case of SCR choppers, commutating circuits have to be incorporated for each main SCR. Such a circuit is described in Chapter 7.

4.6 MODEL OF THE CHOPPER

The chopper is modeled as a first-order lag with a gain of K_{ch}. The time delay corresponds to the statistical average conduction time, which can vary from zero to T. The transfer function is then

$$G_r(s) = \frac{K_r}{1 + \frac{sT}{2}} \tag{4.4}$$

where $K_r = V_s/V_{cm}$, V_s is the source voltage, and V_{cm} is the maximum control voltage.

Increasing the chopping frequency decreases the delay time, and hence the transfer function becomes a simple gain.

4.7 INPUT TO THE CHOPPER

The input to the chopper is either a battery or a rectified ac supply. The rectified ac is the prevalent form of input. The ac input is rectified through a diode bridge, and its output is filtered to keep the dc voltage a constant. The use of the diode bridge has the advantage of near-unity power factor, thus overcoming one of the serious disadvantages of the phase-controlled converter. It has a disadvantage: it cannot transfer power from the dc link into ac mains. In that case, the regenerative energy has to be dumped in the braking resistor, as shown in Figure 4.11, or a phase-controlled converter is connected antiparallel to the diode bridge to handle the regenerative energy, as shown in Figure 4.12. In the latter configuration, the phase-controlled converter can have a smaller rating than other power converters, because the rms value of the regenerative current will be small—the duration of regeneration is only a fraction of the motoring time for most loads.

The regenerating converter has to be operated at triggering angles greater than 90°, to reverse the output dc voltage across the converter to match the polarity of V_s. The phase-controlled converter is enabled only when V_s is greater than the

allowable magnitude ΔV over and above the nominal dc voltage obtained from the ac source. It is usual to set ΔV to be 15 or 20% of V. In such a case, there is a need for a step-up transformer in the path of the phase-controlled converter, to match the dc link voltage V_s. The phase converter is disabled when V_s is slightly greater than 1.35 V, where V is the line-to-line rms voltage, to prevent energy flow from source to dc link and from dc link to source via the phase-controlled converter.

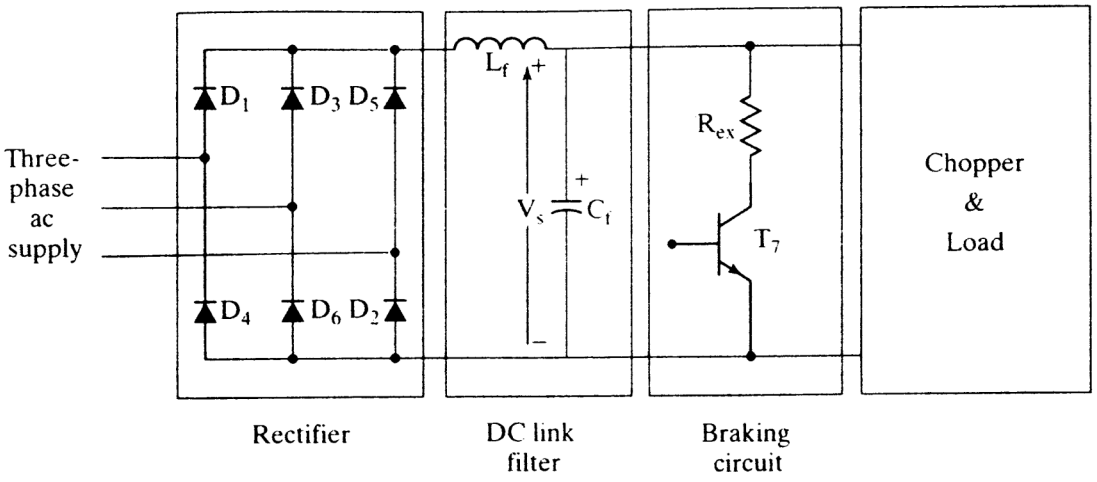

Figure 4.11 Front-end of the chopper circuit

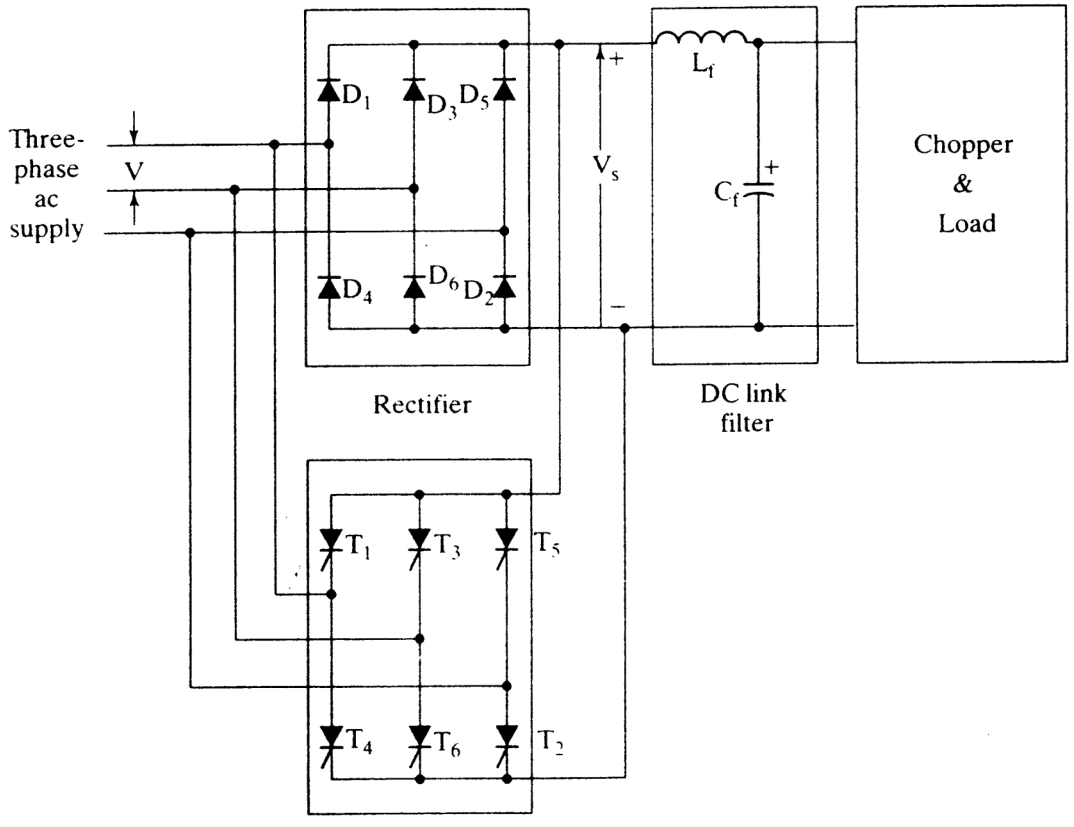

Figure 4.12 Chopper with regeneration capability

4.8 OTHER CHOPPER CIRCUITS

Not all applications demand four-quadrant operation. The power circuit is therefore simplified to accommodate only the necessary operation. Power devices are reduced for one- and two-quadrant drives, resulting in economy of the power converter. Apart from the chopper circuit shown in Figure 4.2 and its variations for reduced quadrants of operation, shown in Figure 4.13, a number of unique

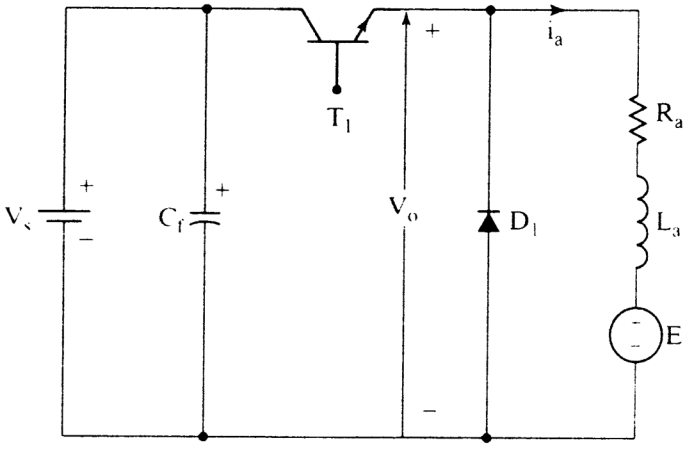

(i) One-quadrant chopper

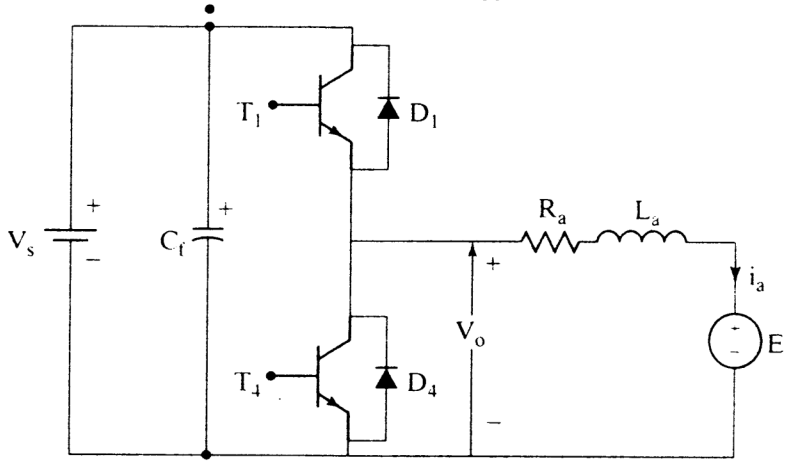

(ii) Two-quadrant chopper

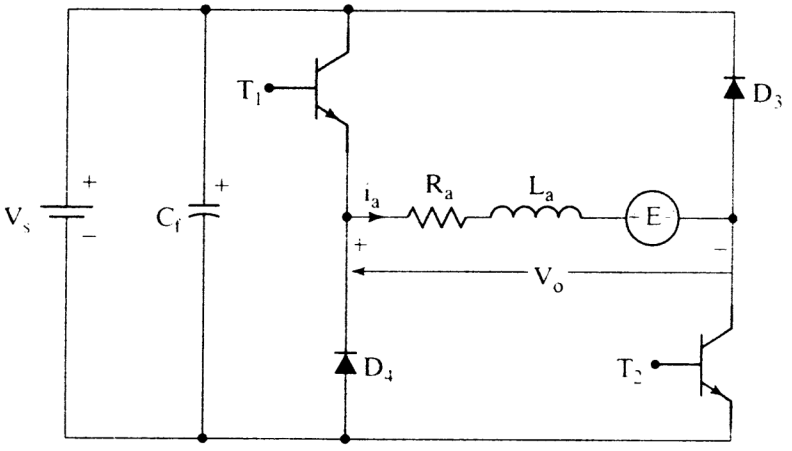

(iii) Two-quadrant chopper

Figure 4.13 Variations of Figure 4.2 for one- and two-quadrant operation

chopper circuits are used. *Morgan* and *Jones* circuits are some of the commonly used choppers for dc motor speed control. They differ in their circuit topologies and commutation of the current from the circuit discussed in this chapter but they all have identical transfer characteristics. Considering this aspect, these circuits are not described and interested readers are referred to power-electronics textbooks.

4.9 STEADY-STATE ANALYSIS OF CHOPPER-CONTROLLED DC MOTOR DRIVE

The steady-state performance of the chopper-controlled dc motor drive is obtained either with average values, by neglecting harmonics, or including harmonics. The justification for using average values is that the average torque is the useful torque that is transmitted to the load. The torque components due to the current harmonics produce an average torque of zero over one cycle of switching. They do not contribute to useful power production. Further, they result in increased armature losses, because the harmonic currents increase the effective motor current. From an output point of view, neglecting harmonics and using only average values gives easier steady-state computation. The analysis by this method is known as *analysis by averaging.*

When losses, maximum steady-state current, and precise electromagnetic torque are required to fully analyze and design the drive system for an application, the true current waveforms in steady state need to be computed. Therefore, the harmonics cannot be excluded in the steady-state computation. A computationally efficient, analytical closed-form expression is obtained by the novel technique of boundary-matching conditions. This method is referred to as *instantaneous steady-state computation.*

It is assumed that the rotor speed is constant and the field is separately excited. For the following analysis, the field flux is maintained at rated value. For any other value of the field flux, the derivations need to be changed only with regard to the induced-emf term.

4.9.1 Analysis by Averaging

The average armature current is

$$I_{av} = \frac{V_{dc} - E}{R_a} \tag{4.5}$$

where

$$V_{dc} = dV_s \tag{4.6}$$

The electromagnetic torque is

$$T_{av} = K_b I_{av} \tag{4.7}$$

The torque, written in terms of duty cycle and speed from equations (4.5), (4.6) and (4.7), is

$$T_{av} = \frac{K_b(dV_s - K_b\omega_m)}{R_a} (N \cdot m) \tag{4.8}$$

The electromagnetic torque is normalized by dividing it by the base torque, T_b, and by dividing both its numerator and denominator by the base voltage, V_b. The normalized torque is obtained by simplifying the expressions and substituting for V_b in terms of the base speed, ω, and emf constant:

$$T_{en} = \frac{T_{av}/V_b}{T_b/V_b} = \frac{K_b(dV_s - K_b\omega_m)/V_b}{K_bI_bR_a/V_b} = \frac{dV_n - \omega_{mn}}{R_{an}}, \text{ p.u.} \tag{4.9}$$

where

$$R_{an} = \frac{I_bR_a}{V_b}, \text{ p.u.} \tag{4.10}$$

$$V_n = \frac{V_s}{V_b}, \text{ p.u.} \tag{4.11}$$

$$\omega_{mn} = \frac{\omega_m}{\omega_b}, \text{ p.u.} \tag{4.12}$$

R_{an}, V_n, and ω_{mn} are normalized resistance, voltage, and speed, respectively. By assigning the product of normalized torque and p.u. resistance on the y axis, a set of normalized performance curves is drawn for various values of duty cycles, normalized voltage, and speed, as is shown in Figure 4.14. From the characteristics and the given duty cycle and voltage, the torque can be evaluated for a given speed, if the normalized resistance is known.

4.9.2 Instantaneous Steady-State Computation

The instantaneous steady-state armature current and electromagnetic torque including harmonics are evaluated in this section, both for continuous and discontinuous current conduction, by boundary-matching conditions. The relevant waveforms are shown in Figure 4.15. For each of the current-conduction modes, the performance is evaluated separately.

4.9.3 Continuous Current Conduction

The relevant electrical equations of the motor for on and off times are as follows:

$$V_s = E + R_ai_a + L_a\frac{di_a}{dt}, \qquad 0 \le t \le dT \tag{4.13}$$

$$0 = E + R_ai_a + L_a\frac{di_a}{dt}, \qquad dT \le t \le T \tag{4.14}$$

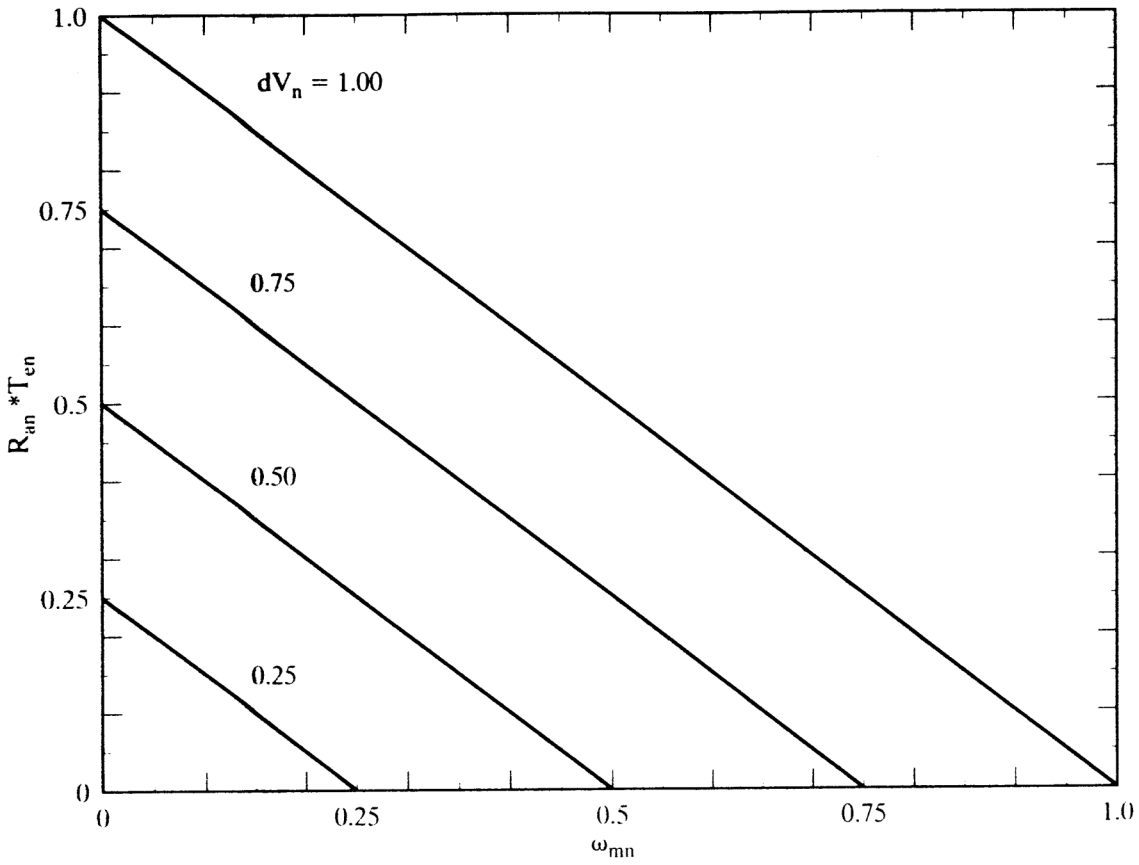

Figure 4.14 Normalized torque–speed characteristics as a function of duty cycle and source voltage

The solution of equation (4.13) is

$$i_a(t) = \frac{V_s - E}{R_a}(1 - e^{\frac{-t}{T_a}}) + I_{a0}e^{-\frac{t}{T_a}}, \qquad 0 < t < dT \tag{4.15}$$

where

$$T_a = \text{Armature time constant} = \frac{L_a}{R_a} \tag{4.16}$$

Similarly, the solution of equation (4.14) is

$$i_a(t) = -\frac{E}{R_a}(1 - e^{-\frac{t'}{T_a}}) + I_{a1}e^{-\frac{t'}{T_a}}, \qquad dT \le t \le dT \tag{4.17}$$

and

$$t' = t - dT \tag{4.18}$$

From Figure 4.15, it is seen that

$$i_a(t) = i_a(t + T) \tag{4.19}$$

By using this boundary condition, I_{a0} and I_{a1} are evaluated as

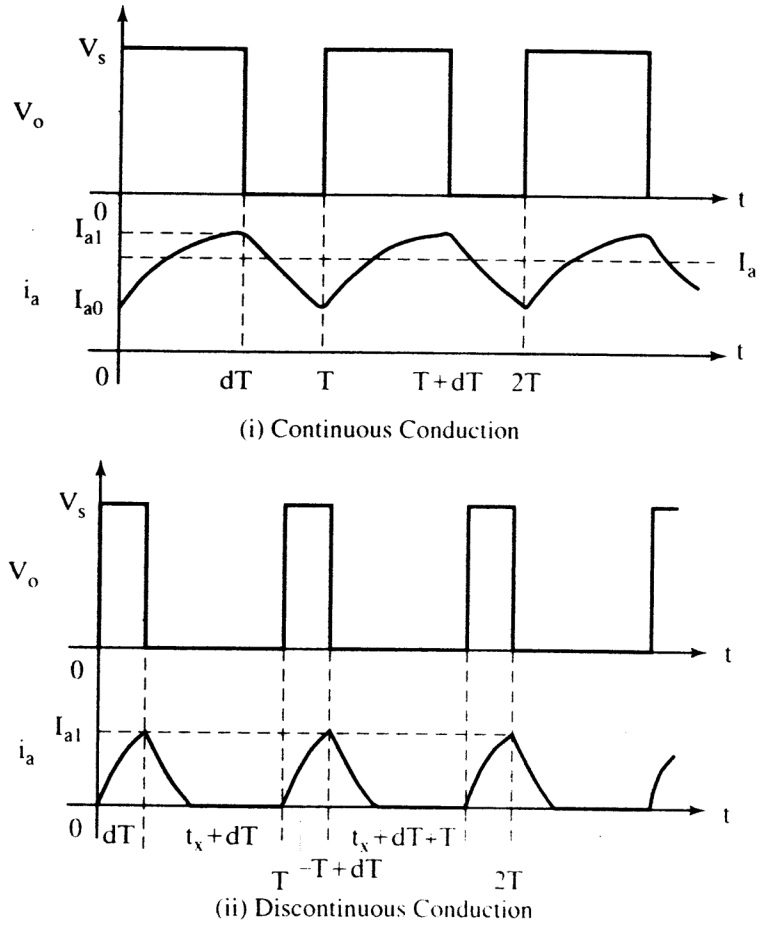

Figure 4.15 Applied voltage and armature current in a chopper-controlled dc motor drive

$$I_{a1} = \frac{V_s(1 - e^{-dT/T_a})}{R_a(1 - e^{-T/T_a})} - \frac{E}{R_a} \tag{4.20}$$

$$I_{a0} = \frac{V_s(e^{dT/T_a} - 1)}{R_a(e^{T/T_a} - 1)} - \frac{E}{R_a} \tag{4.21}$$

Having evaluated I_{a0} and I_{a1}, you can use equations (4.15) and (4.17) to evaluate the instantaneous armature current in steady state.

The limiting or minimum value of duty cycle for continuous current is evaluated by equating I_{a0} to zero. This value is termed the *critical duty cycle*, d_c, and is given by

$$d_c = \left(\frac{T_a}{T}\right)\log_e\left[1 + \frac{E}{V_s}(e^{\frac{T}{T_a}} - 1)\right] \tag{4.22}$$

Duty cycles lower than d_c will produce discontinuous current in the motor. Note that this critical value is dependent on the ratio between chopping time period and armature time constant and also on the ratio between induced emf and source voltage.

4.9.4 Discontinuous Current Conduction

The relevant equations for discontinuous current-conduction mode are obvious from Figure 4.15;

$$V_s = E + R_a i_a + L_a \frac{di_a}{dt}, \qquad 0 < t < dT \tag{4.23}$$

$$0 = E + R_a i_a + L_a \frac{di_a}{dt}, \qquad dT < t < (t_x + dT) \tag{4.24}$$

with

$$i_a(t_x + dT) = 0 \tag{4.25}$$

$$i_a(0) = 0 \tag{4.26}$$

Hence,

$$I_{a1} = \frac{V_s - E}{R_a}(1 - e^{-dT/T_a}) \tag{4.27}$$

$$i_a(t_x + dT) = -\frac{E}{R_a}(1 - e^{-\frac{t_x}{T_a}}) + I_{a1}e^{-\frac{t_x}{T_a}} \tag{4.28}$$

This equation is equal to zero, by the constraint given in equation (4.25), and, from that, t_x is evaluated as

$$t_x = T_a \log_e\left[1 + \frac{I_{a1}R_a}{E}\right] \tag{4.29}$$

The solution for the armature current in three time segments is

$$i_a(t) = \frac{V_s - E}{R_a}(1 - e^{-t/T_a}), \qquad 0 < t < dT \tag{4.30}$$

$$i_a(t) = I_{a1}e^{-\frac{(t-dT)}{T_a}} - \frac{E}{R_a}\left(1 - e^{-\frac{(t-dT)}{T_a}}\right), \qquad dT < t < t_x + dT \tag{4.31}$$

$$i_a(t) = 0, \qquad (t_x + dT) < t < T \tag{4.32}$$

The steady-state performance is calculated by using equations (4.30) to (4.32).

Example 4.1

A dc motor is driven from a chopper with a source voltage of 24V dc and at a frequency of 1 kHz. Determine the variation in duty cycle required to have a speed variation of 0 to 1 p.u. delivering a constant 2 p.u. load. The motor details are as follows:

1 hp, 10 V, 2500 rpm, 78.5 % efficiency, $R_a = 0.01\ \Omega$, $L_a = 0.002$ H, $K_b = 0.03819$ V/rad/sec

The chopper is one-quadrant, and the on-state drop voltage across the device is assumed to be 1 V regardless of the current variation.

Solution **(i)** Calculation of rated and normalized values

$$V_b = 10 \text{ V}$$

$$V_n = \frac{V_s}{V_b} = \frac{24 - 1}{10} = 2.3 \text{ p.u.}$$

$$\omega_{mr} = \frac{2500 \times 2\pi}{60} = 261.79 \text{ rad/sec}$$

$$I_{ar} = \frac{\text{Output}}{\text{Voltage} \times \text{Efficiency}} = \frac{1 \times 746}{10 \times 0.785} = 95 \text{ A} = I_b$$

$$R_{an} = \frac{I_b R_a}{V_b} = \frac{95 \times 0.001}{10} = 0.095 \text{ p.u.}$$

$$T_{en} = 2 \text{ p.u.}$$

(ii) Calculation of duty cycle

The minimum and maximum duty cycles occur at 0 and 1 p.u. speed, respectively, and at 2 p.u. load. From equation (4.9),

$$d = \frac{T_{en}R_{an} + \omega_{mn}}{V_n}$$

$$d_{min} = \frac{2 \times 0.095 + 0}{2.3} = 0.0826$$

$$d_{max} = \frac{2 \times 0.095 + 1}{2.3} = 0.517$$

The range of duty cycle variation required, then, is

$$0.0826 \leq d \leq 0.517$$

Example 4.2

The critical duty cycle can be changed by varying either the electrical time constant or the chopping frequency in the chopper. Draw a set of curves showing the effect of these variations on the critical duty cycle for various values of E/V_s.

Solution

$$d_c = \left(\frac{T_a}{T}\right)\log_e\left[1 + \frac{E}{V_s}\left(e^{\frac{T}{T_a}} - 1\right)\right]$$

In terms of chopping frequency,

$$d_c = f_c T_a \log_e\left[1 + \frac{E}{V_s}\left(e^{\frac{1}{T_a f_c}} - 1\right)\right]$$

Assigning various values of E/V_s and varying f_cT_a would yield a set of critical duty cycles. The graph between d_c and f_cT_a for varying values of E/V_s is shown in Figure 4.16. The maximum value of f_cT_a is chosen to be 10.

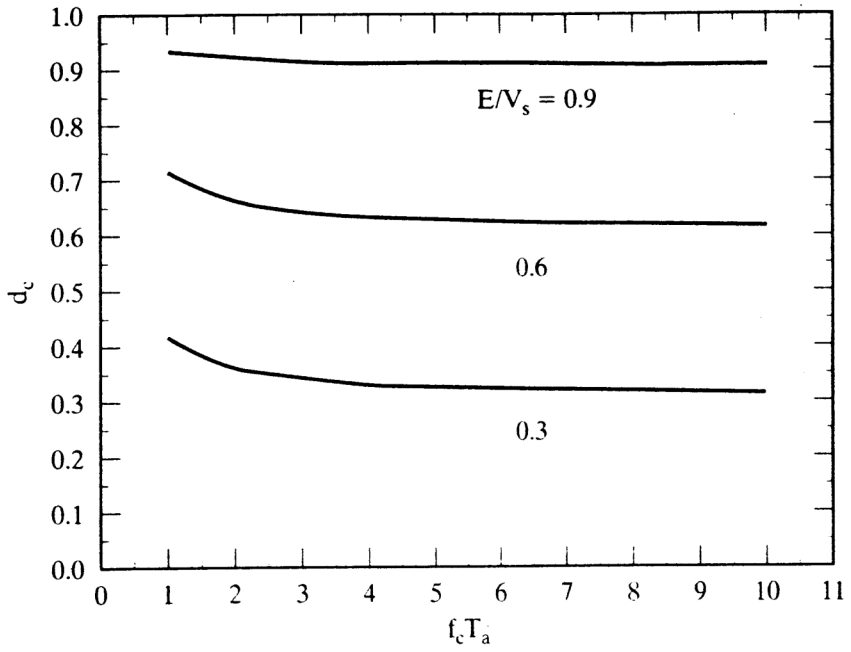

Figure 4.16 Critical duty cycles vs. the product of chopping frequency and electrical time constant of the dc motor, as a function of induced emf and source voltage

Example 4.3

A 200-hp, 230-V, 500-rpm separately-excited dc motor is controlled by a chopper. The chopper is connected to a bridge-diode rectifier supplied from a 230-V, 3-ϕ, 60-Hz ac main. The motor chopper details are as follows:

$$R_a = 0.04\ \Omega,\ L_a = 0.0015\ \text{H},\ K_b = 4.172\text{V/rad/sec},\ f_c = 2\ \text{kHz}.$$

The motor is running at 300 rpm with 55% duty cycle in the chopper. Determine the average current from steady-state current waveform and the electromagnetic torque produced in the motor. Compare these results with those obtained by averaging.

Solution The critical duty cycle is evaluated to determine the current continuity at the given duty cycle of 0.55.

$$d_c = \left(\frac{T_a}{T}\right)\log_e\left[1 + \frac{E}{V_s}\left(e^{\frac{1}{T_a}} - 1\right)\right]$$

$$T_a = \frac{0.0015}{0.04} = 0.0375\ \text{s}$$

$$T = \frac{1}{f_c} = \frac{1}{2 \times 10^3} = 0.5\ \text{ms}$$

$$\frac{T_a}{T} = 75$$

$$V_s = 1.35\ V \cos\alpha = 1.35 \times 230 \times \cos 0^\circ = 310.5\ \text{V}$$

$$E = K_b\omega_m = 4.172 \times \frac{2\pi \times 300}{60} = 131.1\ \text{V}$$

$$d_c = 75\log_e\left[1 + \frac{131.1}{310.5}\left(e^{\frac{1}{75}} - 1\right)\right] = 0.423$$

The given value of d is greater than the critical duty cycle; hence, the armature current is continuous.

$$I_{a0} = \frac{V_s(e^{dT/T_a} - 1)}{R_a(e^{T/T_a} - 1)} - \frac{E}{R_a} = \frac{310.5(e^{0.55/75} - 1)}{0.04(e^{1/75} - 1)} - \frac{131.1}{0.04} = 979 \text{ A}$$

$$I_{a1} = \frac{V_s(1 - e^{-dT/T_a})}{R_a(1 - e^{-T/T_a})} - \frac{E}{R_a} = \frac{310.5(1 - e^{-0.55/75})}{0.04(1 - e^{-1/75})} - \frac{131.1}{0.04} = 1004.7 \text{ A}$$

The average current is

$$I_{av} = \frac{1}{T}\left[\int_0^{dT}\left(\frac{V_s - E}{R_a}(1 - e^{-t/T_a}) + I_{a0}e^{-t/T_a}\right)dt + \int_0^{(1-d)T}\left(-\frac{E}{R_a}(1 - e^{-t/T_a}) + I_{a1}e^{-t/T_a}\right)dt\right]$$

$$= \frac{1}{T}\left[\begin{array}{l} \dfrac{V_s - E}{R_a}\{dT + T_a(e^{-dT/T_a} - 1)\} + I_{a0}T_a(1 - e^{-dT/T_a}) \\ -\dfrac{E}{R_a}\{(1 - d)T - T_a + T_a e^{-(1-d)T/T_a}\} + I_{a1}T_a(1 - e^{-(1-d)T/T_a}) \end{array}\right] = 991.8 \text{ A}$$

$$T_{av} = K_b I_{av} = 4.172 \times 991.8 = 4137.7 \text{ N·m}$$

Steady state by averaging

$$I_{av} = \frac{(dV_s - K_b\omega_m)}{R_a} = \frac{0.55 \times 310.5 - 4.172 \times 31.42}{0.04} = 991.88 \text{ A}$$

$$T_{av} = K_b I_{av} = 4138.1 \text{ N·m}$$

There is hardly any significant difference in the results by these two methods.

4.10 RATING OF THE DEVICES

The chopper shown in Figure 4.2 is considered, for illustration. The armature current is assumed to be continuous, with no ripples. If I_{max} is the maximum allowable current in the dc machine, the rms value of the power switch is dependent on this value and its duty cycle. The duty cycle of one device is slightly more than the duty cycle of the chopper, because one of the power switches continues to carry current during freewheeling while the other is turned off. In order to equal the current loading of the switches, the power switch carrying the freewheeling current is turned off in the next cycle and the previously inactive switch is allowed to carry the freewheeling current alternately. Accordingly, the current waveform of one power switch and the diode is as shown in Figure 4.17. Note that the diodes are, like their respective power switches, alternately carrying the freewheeling current, and only motoring action is considered for the calculation.

The rms value of the power switch current and average diode current are given by,

$$I_t = \sqrt{\frac{I_{max}^2}{2T}(T + dT)} = \sqrt{\frac{1 + d}{2}} \cdot I_{max} \tag{4.33}$$

$$I_d = \left(\frac{1 - d}{2}\right) \cdot I_{max} \tag{4.34}$$

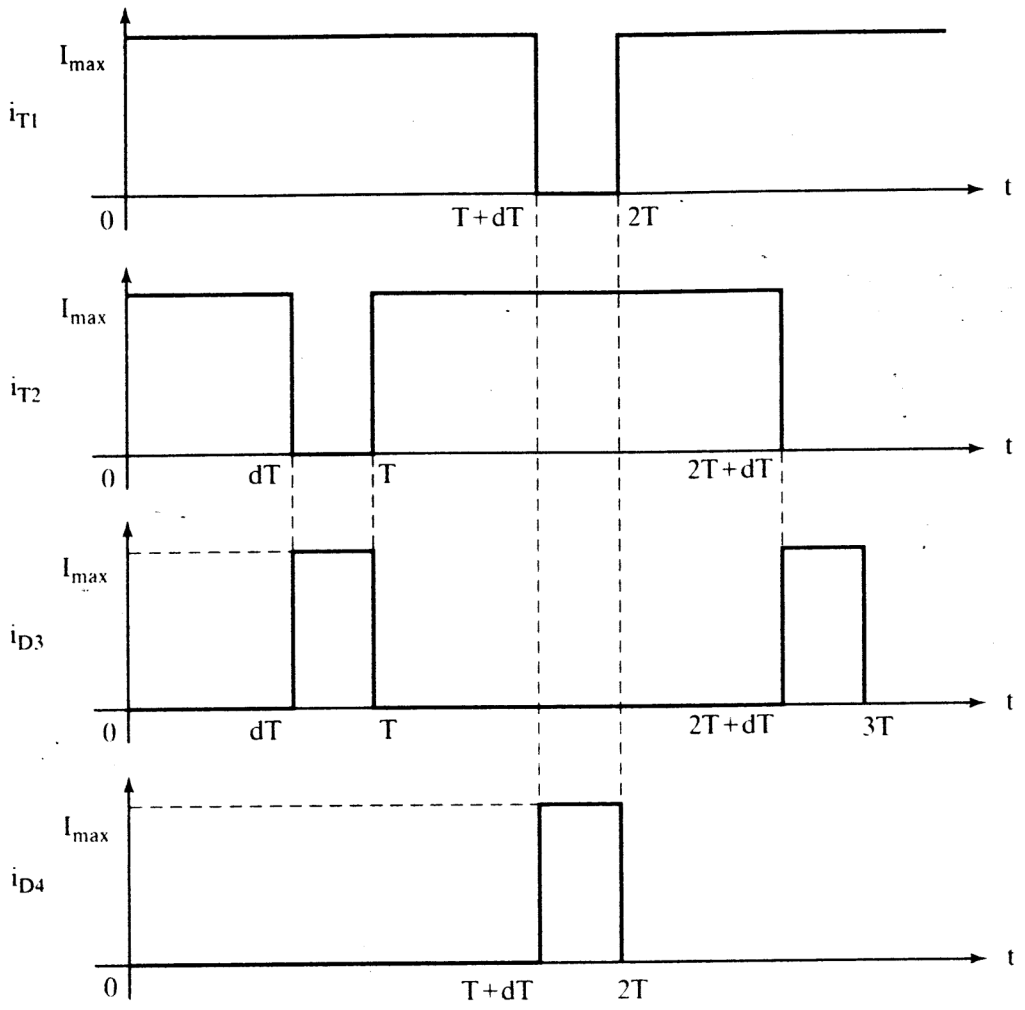

Figure 4.17 Transistor and diode currents in the chopper for motoring operation in the continuous-conduction mode

where the subscripts d and T refer to the diode and power switch, respectively. The average diode and rms power switch currents vs. duty cycle for continuous conduction are shown in Figure 4.18, for design use.

The minimum voltage rating for both the devices is,

$$V_T = V_d = V_s \tag{4.35}$$

Whenever regeneration occurs in the motor drive, the current in the freewheeling diodes would change, and, depending on the frequency and duration of regeneration, the diode currents have to be recalculated. To optimize the chopper rating in comparison to the motor and load demands, the operating conditions have to be known beforehand. The extreme operating conditions would then prevail on the design and hence on the final rating of the chopper.

4.11 PULSATING TORQUES

The armature current has ac components. These ac components or harmonics produce corresponding pulsating torques. The average of the harmonic torques is zero,

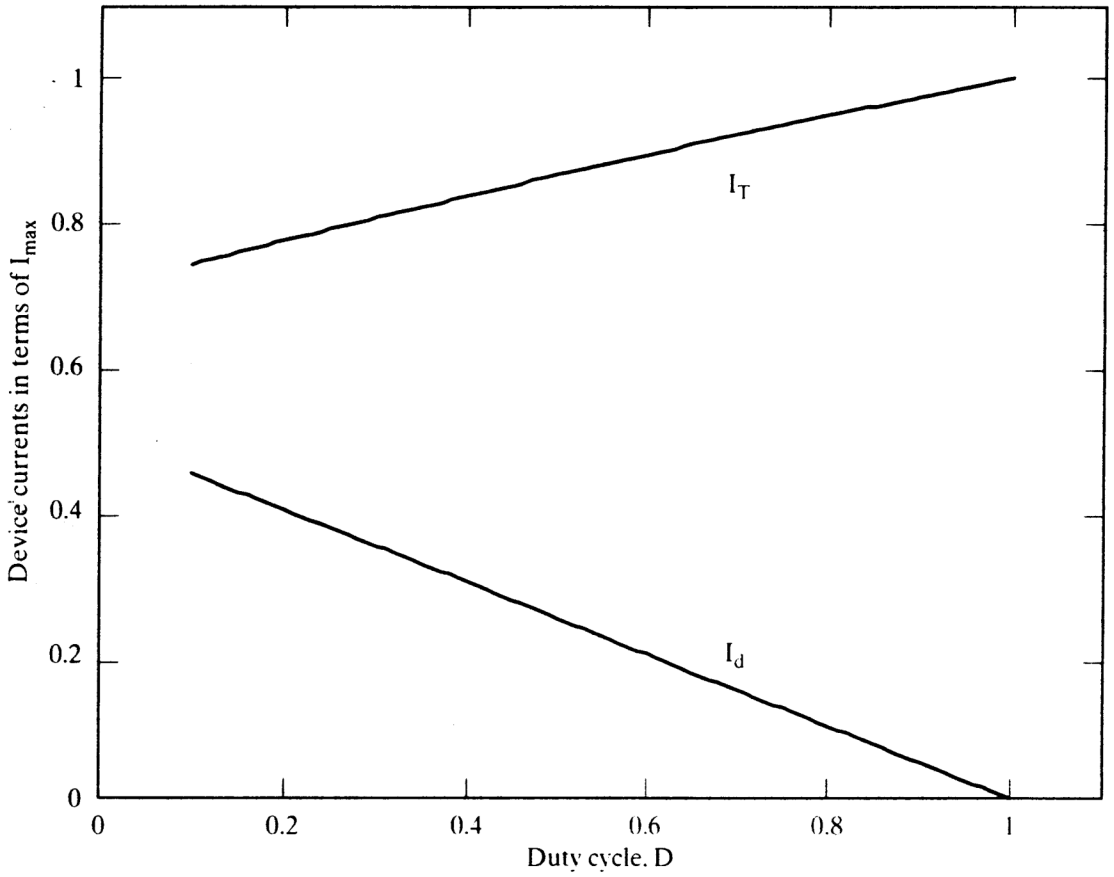

Figure 4.18 Device currents vs. duty cycle for continuous-conduction mode

and they do not contribute to useful torque and power. Some high-performance applications, such as machine tools and robots, require the pulsating torque to be a minimum so as not to degrade the process and the products. In that case, an estimation of the pulsating torques is in order.

The pulsating currents are evaluated from the harmonic voltages and the harmonic armature impedances of the dc machine. The applied voltage shown in Figure 4.10 is resolved into Fourier components as

$$v_a(t) = V_a + \sum_{n=1}^{\infty} A_n \sin(n\omega_c t + \theta_n) \tag{4.36}$$

where

$$V_a = \frac{dT}{T} \cdot V_s = dV_s, \quad V \tag{4.37}$$

$$\omega_c = 2\pi f_c = \frac{2\pi}{T}, \quad \text{rad/sec} \tag{4.38}$$

$$A_n = \frac{2V_s}{n\pi} \sin\frac{n\omega_c dT}{2}, \quad V \tag{4.39}$$

$$\theta_n = \frac{\pi}{2} - \frac{n\omega_c dT}{2}, \quad \text{rad} \tag{4.40}$$

and n is the order of the harmonic. The armature current is expressed as

$$i_a(t) = I_{av} + \sum_{n=1}^{\infty} \frac{A_n}{|Z_n|} \sin(n\omega_c t + \theta_n - \phi_n) \tag{4.41}$$

where

$$I_{av} = \frac{V_a - E}{R_a} \tag{4.42}$$

$$Z_n = R_a + jn\omega_c L_a \tag{4.43}$$

$$\phi_n = \cos^{-1}\left\{\frac{R_a}{\sqrt{R_a^2 + n^2\omega_c^2 L_a^2}}\right\} \tag{4.44}$$

and Z_{an} is the harmonic impedance of the armature. The input power is

$$P_i = v_a(t)i_a(t)$$

$$= \left\{\begin{aligned} &V_a I_{av} + I_{av}\sum_{n=1}^{\infty} A_n \sin(n\omega_c t + \theta_n) + V_a \sum_{n=1}^{\infty} \frac{A_n}{|Z_n|}\sin(n\omega_c t + \theta_n - \phi_n) \\ &+ \sum_{n=1}^{\infty}\left(\frac{A_n^2}{|Z_n|}\sin(n\omega_c t + \theta_n)\sin(n\omega_c t + \theta_n - \phi_n)\right) \end{aligned}\right\} \tag{4.45}$$

The right-hand side of equation (4.45) can be simplified further, because the following pulsating terms reduce to an average of zero.

$$I_{av}\sum_{n=1}^{\infty} A_n \sin(n\omega_c t + \theta_n) = 0 \tag{4.46}$$

$$V_a \sum_{n=1}^{\infty} \frac{A_n}{|Z_n|}\sin(n\omega_c t + \theta_n - \phi_n) = 0 \tag{4.47}$$

The other terms tend to zero, as is shown below.

$$\sum_{n=1}^{\infty}\left(\frac{A_n^2}{|Z_n|}\sin(n\omega_c t + \theta_n)\sin(n\omega_c t + \theta_n - \phi_n)\right)$$

$$= \sum_{n=1}^{\infty}\left(\frac{A_n^2}{|Z_n|}\cdot\frac{1}{2}\{\cos\phi_n - \cos(2n\omega_c t + 2\theta_n - \phi_n)\}\right) \tag{4.48}$$

The average of the double-frequency term is zero, and the power factor is nearly zero because

$$n^2\omega_c^2 L_a^2 >> R_a \tag{4.49}$$

Hence, the expression (4.48) is almost equal to zero. The average input power becomes a constant quantity and is expressed as

$$P_{av} = V_a I_{av} \tag{4.50}$$

Power calculation can use the average values, and there is no need to resort to harmonic analysis, as is shown by the above derivation. The fundamental-harmonic peak pulsating torque then is

$$T_{e1} = K_b i_{a1} \tag{4.51}$$

and the fundamental-harmonic armature current is given by

$$i_{a1} = \frac{2V_s}{\pi\sqrt{R_a^2 + \omega_c^2 L_a^2}} \sin\left(\frac{\omega_c dT}{2}\right) \tag{4.52}$$

The fundamental armature current can be alternately expressed in terms of duty cycle as

$$i_{a1} = \frac{2V_s}{\pi\sqrt{R_a^2 + \omega_c^2 L_a^2}} \sin(\pi d) \tag{4.53}$$

When the duty cycle is 50%, the fundamental armature current, and hence the pulsating torque, is maximum. For a duty cycle of 100%, there are no pulsating-torque components. The instantaneous electromagnetic torque is the sum of the dc and harmonic torques, written as

$$T_e(t) = T_{av} + T_{eh} \tag{4.54}$$

where h is the harmonic order. The harmonic torques, T_{eh}, do not contribute to the load: their averages are zero.

The fundamental pulsating torque is expressed as a fraction of average torque, to examine the impact of duty cycle on the pulsating torque. It is facilitated by the following development.

$$\frac{T_{e1}}{T_{av}} = \frac{K_b i_{a1}}{K_b I_{av}} = \frac{2V_s \sin(\pi d)/(\pi\sqrt{R_a^2 + \omega_c^2 L_a^2})}{(dV_s - E)/R_a} = \frac{2R_a}{\pi\sqrt{R_a^2 + \omega_c^2 L_a^2}} \cdot \frac{V_s}{(dV_s - E)} \sin(\pi d) \tag{4.55}$$

$$= \left(\frac{2}{\pi}\cos\phi_1\right) \frac{\sin(\pi d)}{\left(d - \frac{E}{V_s}\right)} = k_1 \cdot \frac{\sin(\pi d)}{\left(d - \frac{E}{V_s}\right)}$$

where ϕ_1 is the fundamental power-factor angle, which can be extracted from

$$\cos\phi_1 = \frac{R_a}{\sqrt{R_a^2 + \omega_c^2 L_a^2}} \tag{4.56}$$

and

$$k_1 = \frac{2}{\pi}\cos\phi_1 \tag{4.57}$$

A set of normalized curves is shown in Figure 4.19 to indicate the influence of duty cycle and of the ratio between the induced emf and the source voltage on the magnitude of the pulsating torque.

By noting that the fundamental is the predominant component among the ac components, the rms value of the armature current is approximated as

$$I_{rms} = \sqrt{I_{av}^2 + I_1^2} \tag{4.58}$$

where I_1 is the fundamental rms current, given by

$$I_1 = \frac{i_{a1}}{\sqrt{2}} = \frac{\sqrt{2}V_s}{\pi\sqrt{R_a^2 + \omega_c^2 L_a^2}} \sin(\pi d) \tag{4.59}$$

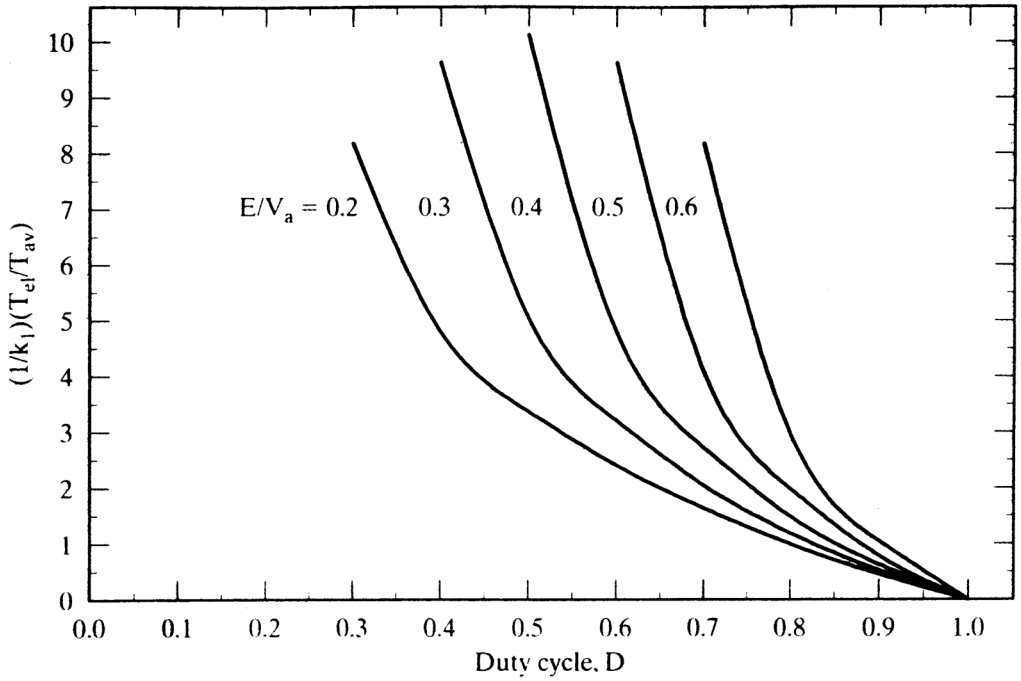

Figure 4.19 Normalized fundamental torque pulsation vs. duty cycle as a function of the ratio between induced emf and source voltage

The armature resistive losses are,

$$P_c = I_{rms}^2 R_a \tag{4.60}$$

This indicates that the thermal capability of the motor is degraded by the additional losses produced by the harmonic currents.

Minimization of the dominant-harmonic torque is of importance in many applications, mainly in positioning of machine tool drives. The key to mitigation of the harmonic torque is revealed by the expression for harmonic current given by equation (4.53). Given a fixed voltage source, there are only two variables that could be utilized to reduce harmonic current: the chopping frequency, and the machine inductance. Note that *d* cannot be used; it is a variable dependent on the speed and load. The chopping frequency is limited by the selection of power device, by its switching losses, and by other factors, such as electromagnetic compatibility. The advantage of varying the carrier frequency is that it is machine-independent, and hence the solution is contained within the chopper. This may not be feasible, as in the case of large (>100 hp) motor drives, but it is possible to increase the armature inductance of the machine during the design of the motor or to include an external inductor to increase the effective inductance in the armature path. The latter solution is the only practical approach in retrofit applications.

Example 4.4

A separately-excited dc motor is controlled by a chopper whose input dc voltage is 180 V. This motor is considered for low-speed applications requiring less than 2% pulsating torque at 300 rpm. (i) Evaluate its suitability for that application. (ii) If it is found unsuit-

able, what is the chopping frequency that will bring the pulsating torque to the specification? (iii) Alternatively, a series inductor in the armature can be introduced to meet the specification. Determine the value of that inductor. The motor and chopper data are as follows:

3 hp, 120 V, 1500 rpm, $R_a = 0.8\ \Omega$, $L_a = 0.003$ H, $K_b = 0.764$ V/rad/sec, $f_c = 500$ Hz

Solution Rated torque,

$$T_{er} = \frac{3 \times 745.6}{2\pi \times 1500/60} = 14.25\ \text{N}\cdot\text{m}$$

Maximum pulsating torque permitted $= 0.02 \times T_{er} = 0.02 \times 14.25 = 0.285\ \text{N}\cdot\text{m}$

To find the harmonic currents, it is necessary to know the duty cycle. That is approximately determined by the averaging-analysis technique, by assuming that the motor delivers rated torque at 300 rpm.

$$I_b = \frac{T_{er}}{K_b} = \frac{14.25}{0.764} = 18.65\ \text{A}$$

$$V_a = E + I_{av}R_a = K_b\omega_m + I_{av}R_a = 0.764 \times \frac{2\pi \times 300}{60} + 18.65 \times 0.8 = 38.91\ \text{V}$$

$$d = \frac{V_a}{V_s} = \frac{38.91}{180} = 0.216$$

(i) The fundamental pulsating torque is assumed to be predominant for this analysis.

$$i_{a1} = \frac{2V_s}{\pi\sqrt{R_a^2 + \omega_c^2 L_a^2}} \sin(\pi d) = \frac{2 \times 180}{\pi\sqrt{0.8^2 + (2\pi \times 500 \times 0.003)^2}} \sin(0.216\pi) = 7.6\ \text{A}.$$

$$T_{e1} = K_b i_{a1} = 0.764 \times 7.6 = 5.8\ \text{N}\cdot\text{m}$$

This pulsating torque exceeds the specification, and, hence, in the present condition, the drive is unsuitable for use.

(ii) The fundamental current to produce 2% pulsating torque is

$$i_{a1(spec.)} = \frac{T_{e1(spec)}}{K_b} = \frac{0.285}{0.764} = 0.373\ \text{A}$$

$$i_{a1(spec.)} = \frac{2V_s}{\pi\sqrt{R_a^2 + \omega_c^2 L_a^2}} \sin(\pi d)$$

from which the angular switching frequency to meet the fundamental current specification is obtained as

$$\omega_{c1} = \sqrt{\frac{4V_s^2 \sin^2(\pi d)}{\pi^2 L_a^2 i_{a1(spec.)}^2} - \frac{R_a^2}{L_a^2}} = \sqrt{(4 \times 180^2 \sin^2(0.216\pi)/(\pi^2(0.003)^2(0.373)^2) - \left(\frac{0.8}{0.003}\right)^2}$$

$$= 64.278\ \text{rad/s}$$

$$f_{c1} = \frac{\omega_{c1}}{2\pi} = 10.23\ \text{kHz}$$

Note that f_{cl} is the chopping frequency in Hz, which decreases the pulsating torque to the specification.

(iii) Let L_{ex} be the inductor introduced in the armature circuit. Then its value is

$$L_{ex} = \sqrt{\frac{4V_s^2\sin^2(\pi d)}{\pi^2\omega_c^2 i_{al(spec)}^2} - \frac{R_a^2}{\omega_c^2}} - L_a$$

$$= \sqrt{(4 \times 180^2 \sin^2(0.216\pi))/(\pi^2(2\pi \times 500)^2(0.373)^2) - \left(\frac{0.8}{2\pi \times 500}\right)^2} - 0.003 = 71.5 \text{ mH}$$

Example 4.5

Calculate (i) the maximum harmonic resistive loss and (ii) the derating of the motor drive given in Example 4.4. The motor is operated with a base current of 18.65 A, which is inclusive of the fundamental-harmonic current. Consider only the dominant-harmonic component, to simplify the calculation.

Solution

$$I_{rms}^2 = I_b^2 = I_{av}^2 + I_1^2$$

By dividing by the square of the base current, the equation is expressed in terms of the normalized currents as

$$I_{avn}^2 + I_{1n}^2 = 1 \text{ p.u.}$$

where

$$I_{1n} = \frac{\sqrt{2}}{\pi}\frac{V_s}{\sqrt{R_a^2 + \omega_c^2 L_a^2}}\sin(\pi d)\frac{1}{I_b} = \frac{\sqrt{2}}{\pi}\frac{V_{sn}}{Z_{an}}\sin(\pi d)$$

where

$$V_{sn} = \frac{V_s}{V_b}; Z_{an} = \frac{Z_a}{Z_b} = \frac{\sqrt{R_a^2 + \omega_c^2 L_a^2}}{Z_b}$$

$$Z_b = \frac{V_b}{I_b} = \frac{120}{18.65} = 6.43\ \Omega$$

$$V_{sn} = \frac{180}{120} = 1.5 \text{ p.u.}$$

$$Z_a = \sqrt{0.8^2 + (2\pi * 500 * 0.003)^2} = 9.42\ \Omega$$

$$Z_{an} = \frac{9.42}{6.43} = 1.464 \text{ p.u.}$$

For a duty cycle of 0.5, the dominant-harmonic current is maximum and is given as

$$I_{1n} = \frac{\sqrt{2}}{\pi}\frac{1.5}{1.464} = 0.46 \text{ p.u.}$$

(i) The dominant-harmonic armature resistive loss is

$$P_{1n} = I_{1n}^2 R_{an} = 0.46^2 \frac{0.8}{6.43} = 0.02628 \text{ p.u.}$$

(ii) For equality of losses in the machine with pure and chopped-current operation, the average current in the machine with chopped-current operation is derived as

$$I_{avn} = \sqrt{1 - I_{in}^2} = \sqrt{1 - .46^2} = 0.887 \text{ p.u.}$$

which translates into an average electromagnetic torque of 0.887 p.u., resulting in 11.3% derating of the torque and hence of output power.

4.12 CLOSED-LOOP OPERATION

4.12.1 Speed-Controlled Drive System

The speed-controlled dc-motor chopper drive is very similar to the phase-controlled dc-motor drive in its outer speed-control loop. The inner current loop and its control are distinctly different from those of the phase-controlled dc motor drive. This difference is due to the particular characteristics of the chopper power stage. The current loop and speed loop are examined, and their characteristics are explained, in this section. The closed-loop speed-controlled separately-excited dc motor drive is shown in Figure 4.20 for analysis, but the drive system control strategy is equally applicable to a series motor drive.

4.12.2 Current Control Loop

With inner current loop alone, the motor drive system is a torque amplifier. The commanded value of current is compared to the actual armature current, and its error is processed through a current controller. The output of the current controller, in conjunction with other constraints, determines the base drive signals of the chopper switches. The current controller can be either of the following types:

(i) Pulse-Width-Modulation (PWM) controller

(ii) Hysteresis controller

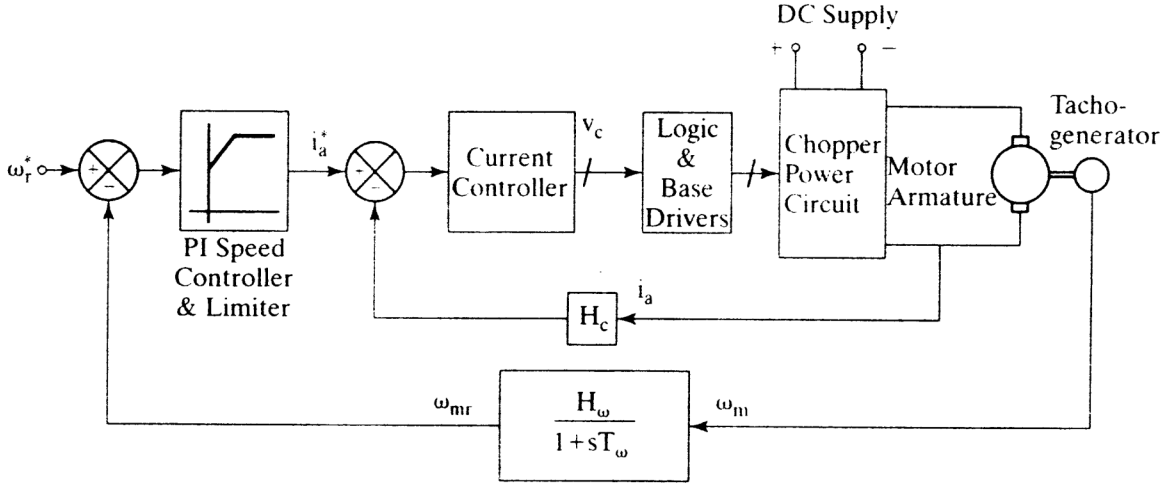

Figure 4.20 Speed-controlled dc-motor chopper drive

The selection of the current controller affects its transient response (and hence the overall speed loop bandwidth indirectly). These two controllers are described in the following sections.

4.12.3 Pulse-Width-Modulated Current Controller

The current error is fed into a controller, which could be proportional (P), proportional plus integral (PI), or proportional, integral, and differential (PID). The most commonly used controller among them is the PI controller. The current error is amplified through this controller and emerges as a control voltage, v_c. It is required to generate a proportional armature voltage from the fixed source through a chopper operation. Therefore, the control voltage is equivalent to the duty cycle of the chopper. Its realization is as follows. The control voltage is compared with a ramp signal to generate the on- and off-times, as shown in Figure 4.21. *On* signal is produced if the control voltage is greater than the ramp (carrier) signal; *off* signal is generated when the control signal is less than the ramp signal.

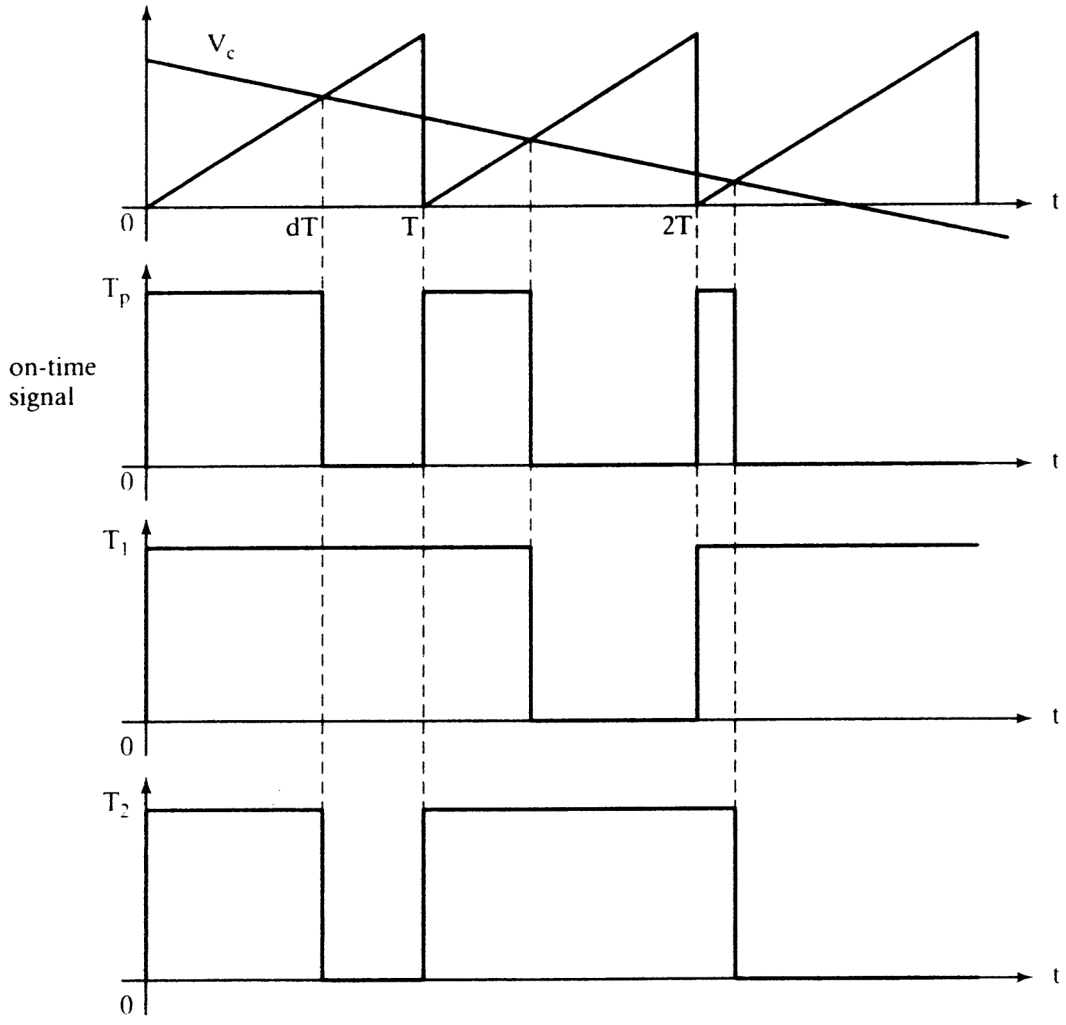

Figure 4.21 Generation of base-drive signals from current error for forward motoring when one is using the chopper shown in Figure 4.2

This logic amounts to the fact that the duration for which the control signal exceeds the ramp signal determines the duty cycle of the chopper. The on- and off-time signals are combined with other control features, such as interlock, minimum on- and off-times, and quadrant selection. The interlock feature prevents the turning on of the transistor (top/bottom) in the same leg before the other transistor (bottom/top) is turned off completely. This is ensured by giving a time delay between the turn-off instant of one device and the turn-on instant of the other device in the same phase leg. Simultaneous conduction of the top and bottom devices in the same leg results in a short circuit of the dc source; it is known as shoot-through failure in the literature.

Figure 4.21 corresponds to the forward motoring operation in the four-quadrant chopper shown in Figure 4.2. When the motor drive is to operate in the third and fourth quadrants, the armature current reverses. This calls for a change in the current-control circuitry. A block diagram of the current controller is shown in Figure 4.22, including all the constraints pertaining to the operational quadrant. The speed and current polarities, along with that of the control voltage, determine the quadrant and hence the appropriate gating signals. The on-time is determined by comparing the ramp signal with the absolute value of the control voltage. The current-error signal, which determines the control voltage v_c, is rectified to find the intersection point between the carrier ramp and v_c. A unidirectional carrier-ramp signal can be used when the control voltage is also unidirectional, but the control voltage will be negative when the current error becomes negative. It happens for various cases, such as reducing the reference during transient operation and changing the polarity of the reference to go from quadrant one to three or four. Taking the polarity of the control voltage and

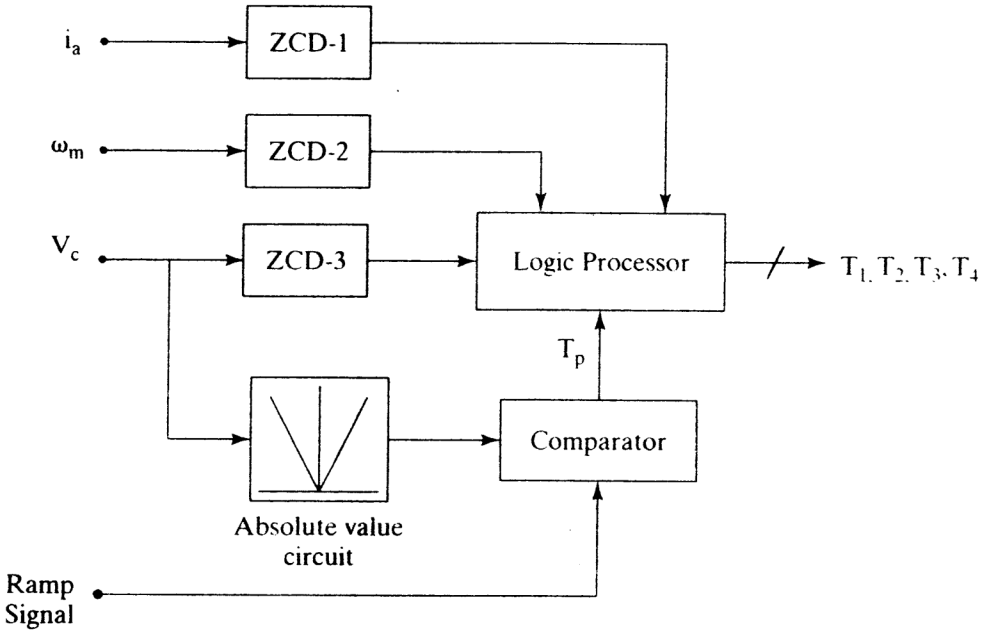

Note : ZCD — Zero Crossing Detector for polarity detection

Figure 4.22 PWM current-controller implementation with ramp carrier signal

combining it with the polarities of the current and speed gives the operational quadrant. The chopper *on* and *off* pulses generated with the intersection of rectified v_c and carrier ramp will then be combined with the quadrant-selector signals of speed, current, and control-voltage polarities to generate the base-drive signals to the chopper switching devices. An illustration is given in the drive-system simulation section.

Instead of a ramp signal for carrier waveform, a unidirectional sawtooth waveform could be used. It is advantageous in that it has symmetry between the rising and falling sides of the waveform, unlike the ramp signal. Its principle of operation is explained in the following.

The voltage applied to the load is varied within one cycle of the carrier signal. This is illustrated in Figure 4.23. The switching logic is summarized as follows:

$$i_a^* - i_a \geq \text{carrier frequency saw tooth waveform magnitude}, T_p = 1, v_a = V_s \quad (4.61)$$

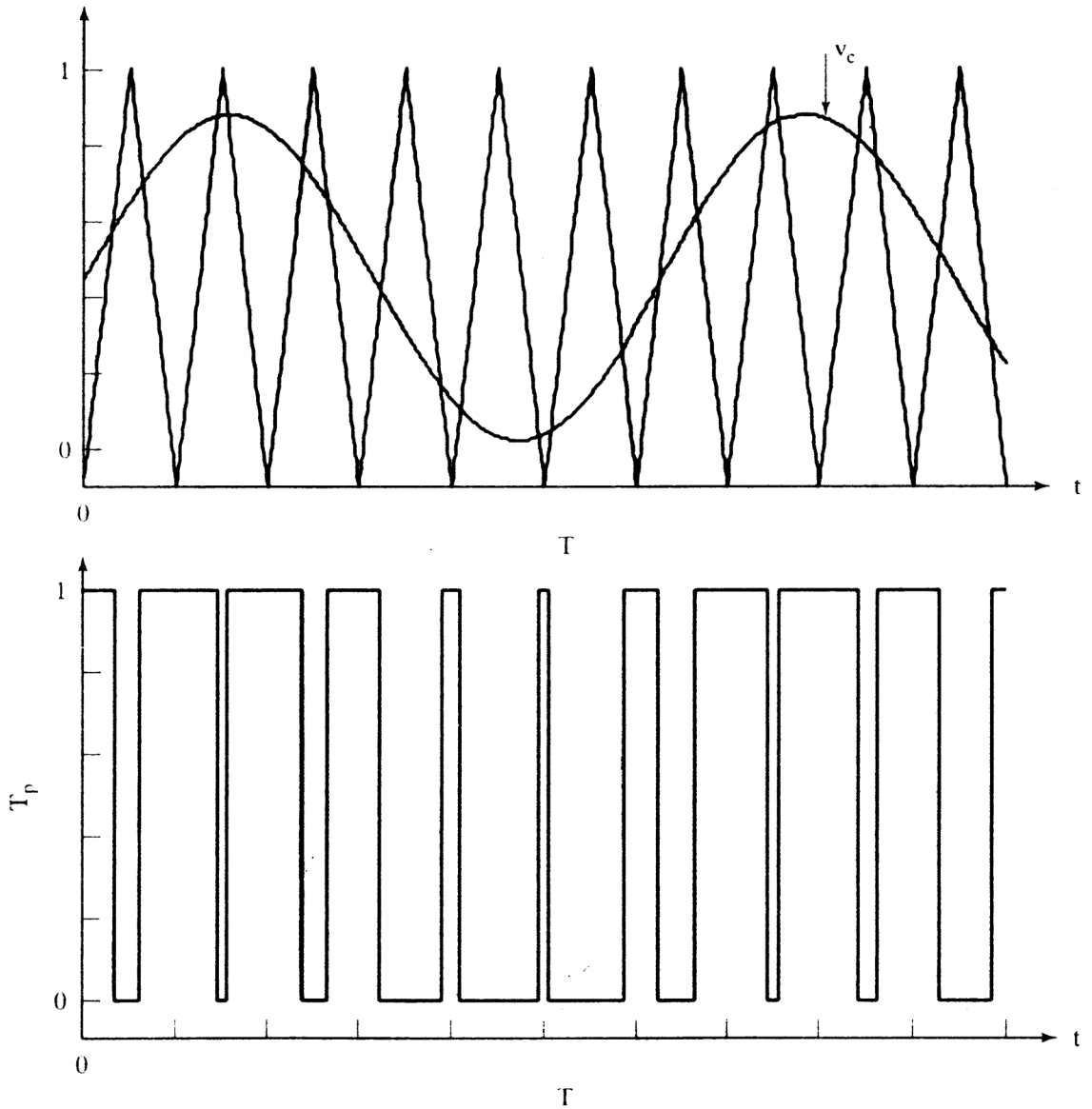

Figure 4.23 Principle of PWM operation

$i_a^* - i_a <$ carrier frequency saw tooth waveform magnitude, $T_p = 0$, $v_a = 0$ (4.62)

For a fast response, the current error is amplified so that a small current error would activate the chopper control. The PWM controller has the advantage of smaller output ripple current for a given switching frequency, compared to the hysteresis current controller described later.

The pulses generated from the PWM controller are substituted for T_p in the block diagram shown in Figure 4.22. They are then processed for quadrant selection, interlock, and safety features, and appropriate base-drive signals are generated for application to the chopper circuit.

4.12.4 Hysteresis-Current Controller

The PWM current controller acts once a cycle, controlling the duty cycle of the chopper. The chopper then is a variable voltage source with average current control. Instantaneous current control is not exercised in the PWM current controller. In between two consecutive switchings, the current can exceed the maximum limit; if the PWM controller is sampled and held once a switching cycle, then the current is controlled on an average but not on an instantaneous basis. The hysteresis controller overcomes such a drawback by converting a voltage source into a fast-acting current source. The current is controlled within a narrow band of excursion from its desired value in the hysteresis controller. The hysteresis window determines the allowable or preset deviation of current, Δi. Commanded current and actual current are shown in Figure 4.24 with the hysteresis windows. The voltage applied to the load is determined by the following logic:

$$i_a \leq i_a^* - \Delta i, \quad \text{set } v_a = V_s \tag{4.63}$$

$$i_a \geq i_a^* + \Delta i, \quad \text{reset } v_a = 0 \tag{4.64}$$

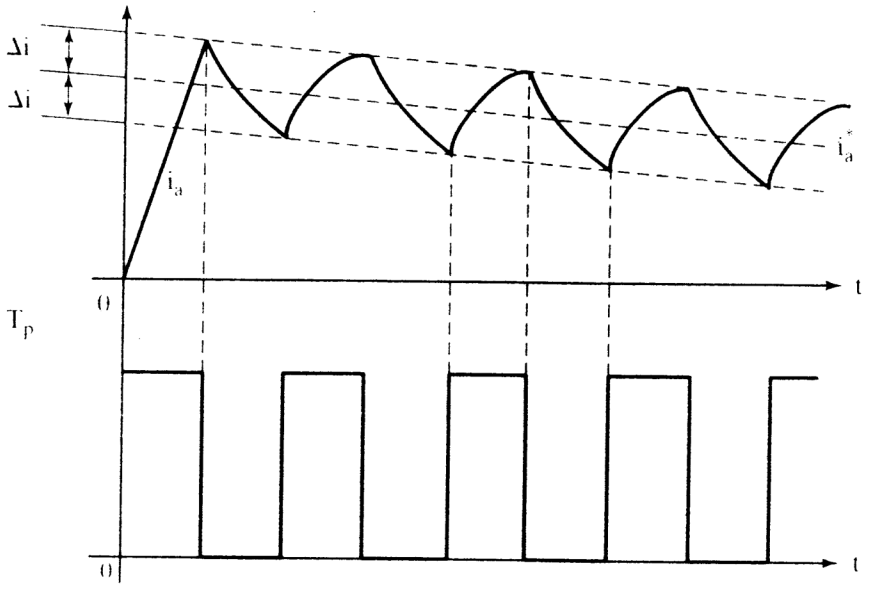

Figure 4.24 Hysteresis-controller operation

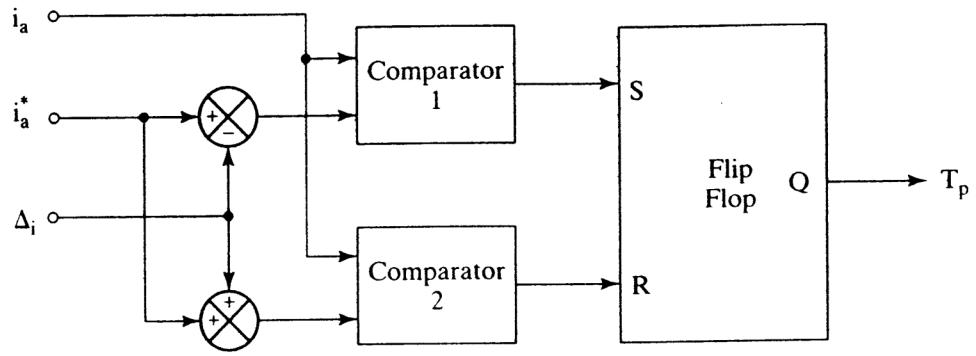

Figure 4.25 Realization of hysteresis controller

TABLE 4.1 Comparison of current controllers

Characteristics	Current Controllers	
	Hysteresis	PWM
Switching Frequency	Varying	Fixed at Carrier Frequency
Speed of Response	Fastest	Fast
Ripple Current	Adjustable	Fixed
Filter Size	Dependent on Δi	Usually small
Switching Losses	Usually high	Low

The realization of this logic is shown in Figure 4.25. The window, Δi, can either be externally set as a constant or be made a fraction of armature current, by proper programming. The chopping frequency is a varying quantity, unlike the constant frequency in the PWM controller. This has the disadvantage of higher switching losses in the devices with increased switching frequency.

The T_p pulses issued from the hysteresis controller replace the block consisting of the comparator output in the Figure 4.22. All other features remain the same for the implementation of the hysteresis controller. This controller provides the fastest response, by means of its instantaneous action. A qualitative comparison of the PWM and hysteresis controllers is summarized in Table 4.1.

4.12.5 Modeling of Current Controllers

The current-error amplifier is modeled as a gain and is given by

$$G_c(s) = K_c \tag{4.65}$$

The chopper is modeled as a first-order lag, with a gain given by

$$G_r(s) = \frac{K_r}{\left(1 + \frac{sT}{2}\right)} \tag{4.66}$$

The PWM current controller has a delay of half the time period of the carrier waveform, and its gain is that of the chopper. Hence, its transfer function, including that of the chopper, is

$$G_c G_r(s) = \frac{K_c K_r}{\left(1 + \frac{sT}{2}\right)} \tag{4.67}$$

where K_c is the gain of the PWM current controller, K_r is the gain of the chopper, and the time constant T is given by,

$$T = \frac{1}{\text{carrier frequency}} = \frac{1}{f_c} \tag{4.68}$$

The gain of the PWM current controller is dependent on the gain of the current-error amplifier. For all practical purposes, the PWM current control loop can be modeled as a unity-gain block if the delay due to the carrier frequency is negligible.

The hysteresis controller has instantaneous response; hence, the current loop is approximated as a simple gain of unity.

4.12.6 Design of Current Controller

The current loop is not easily approximated into a first-order transfer function, unlike the case of the phase-controlled-rectifier drive system. The chopping frequency is considered to be high enough that the time constant of the converter is very much smaller than the electrical time constants of the dc motor. That leads to the converter model given by the product of the converter and current-controller gains. Then the closed-loop current-transfer function is written as

$$\frac{i_a(s)}{i_a^*(s)} = K_c K_r K_1 \frac{(1 + sT_m)}{(1 + sT_1)(1 + sT_2) + H_c K_r K_c K_1 (1 + sT_m)} \tag{4.69}$$

where $K_1 = \dfrac{B_t}{K_b^2 + R_a B_t}$ and K_c and K_r are the current-controller and chopper gains, respectively. The chopper gain is derived as

$$K_r = \frac{V_s}{V_{cm}} \tag{4.70}$$

where V_s is the dc link voltage and V_{cm} is the maximum control voltage.

The gain of the current controller is not chosen on the basis of the damping ratio, because the poles are most likely to be real ones. Lower the gain of the current controller; the poles will be far removed from the zero. The higher the value of the gain, the closer will one pole move to the zero, leading to the approximate cancellation of the zero. The other pole will be far away from the origin and will contribute to the fast response of the current loop. Consider the worked-out Example 3.4 from the previous chapter. The values of various constants are :

$$K_1 = 0.049 \quad H_c = 0.355 \quad T_m = 0.7 \quad T_1 = 0.1077$$
$$T_2 = 0.0208 \quad V_s = 285\ \text{V} \quad V_{cm} = 10\text{V} \quad K_r = 28.5\ \text{V}$$

The zero of the closed current-loop transfer function is at -1.42. Note that this is not affected by the current controller. The closed-loop poles for current-controller gains of 0.1, 1, and 10 are given below, along with their steady-state gains, in the following table.

K_c	Poles	Steady-state gain
0.1	$-7.18, -65.11$	21.33
1.0	$-3.24, -203.45$	213.38
10.0	$-1.66, -1549.0$	2580.30

It is seen that, as the gain increases, one of the poles moves closer to the zero at $-\frac{1}{T_m}$, enabling cancellation and a better dynamic response.

In high-performance motor-drive systems, it is usual to have a PI current controller instead of the simple proportional controller illustrated in this section. The PI controller provides zero steady-state current error, whereas the proportional controller will have a steady-state error. In the case of the PI current controller, the design procedure for the phase-controlled dc motor-drive system can be applied here without any changes. The interested reader can refer to Chapter 3 for further details on the design of the PI current controller.

4.12.7 Design of Speed Controller by the Symmetric-Optimum Method

The block diagram for the speed-controlled drive system with the substitution of the current-loop transfer function is shown in Figure 4.26. Assuming that the time constant of the speed filter is negligible, the speed-loop transfer function is derived from Figure 4.26 as

$$\frac{\omega_m(s)}{\omega_r^*(s)} = \frac{1}{H_\omega} \cdot \frac{a_0(1 + sT_s)}{a_0 + a_1 s + a_2 s^2 + a_3 s^3} \tag{4.71}$$

where

$$a_0 = K_5 \frac{K_s}{T_s} \tag{4.72}$$

$$a_1 = 1 + H_c K_r K_c K_1 + K_5 K_s \tag{4.73}$$

$$a_2 = T_1 + T_2 + H_c K_r K_c K_1 T_m \tag{4.74}$$

$$a_3 = T_1 T_2 \tag{4.75}$$

$$K_5 = K_b \frac{H_\omega K_r K_c K_1}{B_t} \tag{4.76}$$

This is very similar to the equation derived in Chapter 3, from which the following symmetric optimum conditions are imposed:

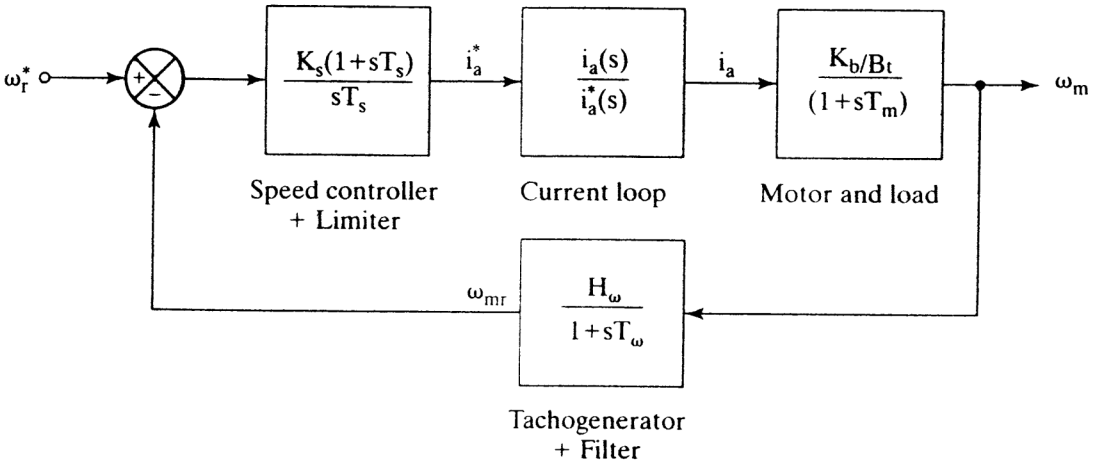

Figure 4.26 Simplified speed-controlled dc motor drive fed from a chopper with hysteresis-current control

$$a_1^2 = 2a_0a_2 \tag{4.77}$$

$$a_2^2 = 2a_1a_3 \tag{4.78}$$

Conditions given by equations (4.77) and (4.78) result in speed-controller time and gain constants given by

$$K_s = \frac{1}{K_5} \cdot \left\{ \frac{a_2^2}{2a_3} - (1 + H_cK_rK_cK_1) \right\} \tag{4.79}$$

$$T_s = \frac{2K_5K_sa_2}{a_1^2} \tag{4.80}$$

For the same example, the speed-controller gain and time constants for various gains of the current controller are given next, together with the closed-loop poles and zeros and the steady-state gains of the speed-loop transfer function.

Current controller gain	Speed controller gain	Speed controller time constant	Steady-state gain	Zero	Poles
0.1	106.7	0.045	1628	−22.22	−18.3 ± j31, −36.9
1.0	102.9	0.0188	38,000	−53.2	−52.7 ± j88.9, −105.1
10.0	597.0	0.0026	1.6×10^7	−384.6	−393 ± j666.8, −792.4

Increasing current-controller gain has drastically reduced the speed-loop time constant without appreciably affecting the damping ratio of the closed-loop speed-control system. Because of the large integral gain in the speed controller, its output will saturate in time. An anti-windup circuit is necessary to overcome the saturation in this controller design and thus to keep the speed controller responsive. The anti-windup circuit can be realized in many ways. One of the implementations is shown in Figure 4.27.

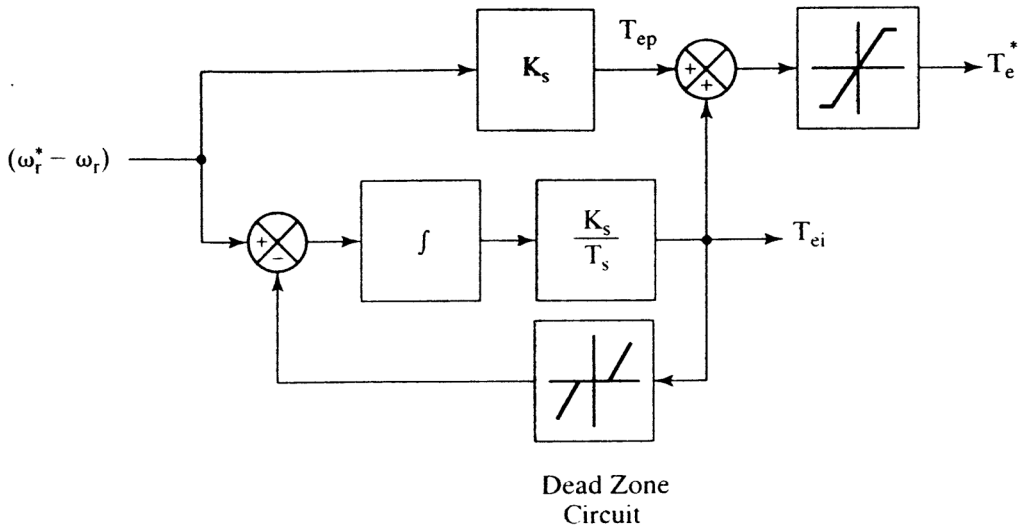

Figure 4.27 Anti-windup circuit with PI speed controller

The saturation due to the integral action alone is countered in this implementation. It is achieved by a negative-feedback control of the integral-controller output through a dead-zone circuit. This dead-zone circuit produces an output only when the integral controller output exceeds a preset absolute maximum, i.e., when the controller output saturates. This feedback is subtracted from the speed error and the resulting signal constitutes the input to the integrator. When the integral-controller output saturates, the input to the integral controller is reduced. This action results in the reduction of the integral controller's output, thus pulling the integral controller from saturation and making the controller very responsive. If there is no saturation of the integral-controller output, then the feedback is zero (because of the dead-zone circuit); hence, the anti-windup circuit is inactive in this implementation. The outputs of the integral and the proportional controllers are summed, then limited, to generate the torque reference signal. By keeping the outputs of the proportional and integral controllers separate, their individual tuning and the beneficial effect of the high proportional gain are maintained.

4.13 DYNAMIC SIMULATION OF THE SPEED-CONTROLLED DC MOTOR DRIVE

A dynamic simulation is recommended before a prototype or an actual drive system is built and integrated, to verify its capability to meet the specifications. Such a simulation needs to consider all the motor-drive elements, with nonlinearities. The transfer-function approach could become invalid, because of the nonlinear current loop. This drawback is overcome with the time-domain model developed below. The speed-controlled drive shown in Figure 4.20, but modified to include the effects of field excitation variation and with a PWM or a hysteresis controller, is considered for the simulation.

4.13.1 Motor Equations

The dc motor equations, including its field, are

$$V_a = R_a i_a + L_a \frac{di_a}{dt} + K\Phi_f \omega_m \tag{4.81}$$

$$V_f = R_f i_f + L_f \frac{di_f}{dt} \tag{4.82}$$

$$T_e - T_l = J\frac{d\omega_m}{dt} + B_l \omega_m \tag{4.83}$$

$$T_e = K\Phi_f i_a \tag{4.84}$$

where

$$K\Phi_f = Mi_f \tag{4.85}$$

and M is the mutual inductance between the armature and field windings.

The state variables are defined as

$$x_1 = i_a \tag{4.86}$$

$$x_2 = \omega_m \tag{4.87}$$

$$x_3 = i_f \tag{4.88}$$

The motor equations in terms of the state variables are

$$\dot{x}_1 = -\frac{R_a}{L_a}x_1 - \frac{M}{L_a}x_2 x_3 + \frac{1}{L_a}V_a \tag{4.89}$$

$$\dot{x}_2 = \frac{M}{J}x_1 x_3 - \frac{B_l}{J}x_2 - \frac{T_l}{J} \tag{4.90}$$

$$\dot{x}_3 = -\frac{R_f}{L_f}x_3 + \frac{1}{L_f}V_f \tag{4.91}$$

4.13.2 Speed Feedback

The tachogenerator and the filter are combined in the transfer function as

$$\frac{\omega_{mr}(s)}{\omega_m(s)} = \frac{H_\omega}{1 + sT_\omega} \tag{4.92}$$

The state diagram of equation (4.92) is shown in Figure 4.28, where

$$x_4 = \omega_{mr} \tag{4.93}$$

and the state equation is obtained from the state diagram as

$$\dot{x}_4 = \frac{I}{T_\omega}(H_\omega x_2 - x_4) \tag{4.94}$$

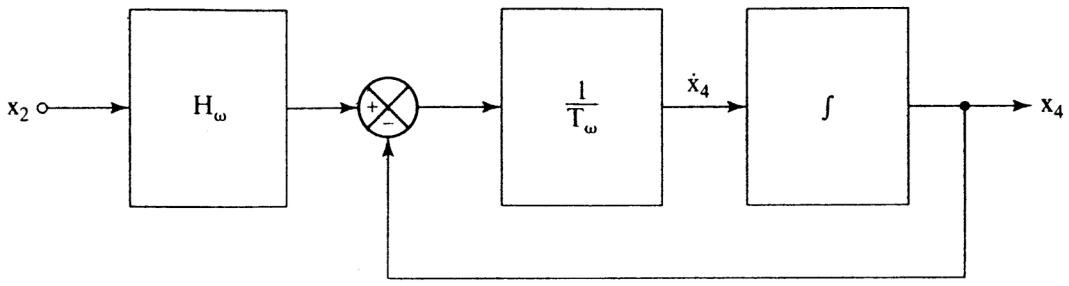

Figure 4.28 State diagram of the speed feedback

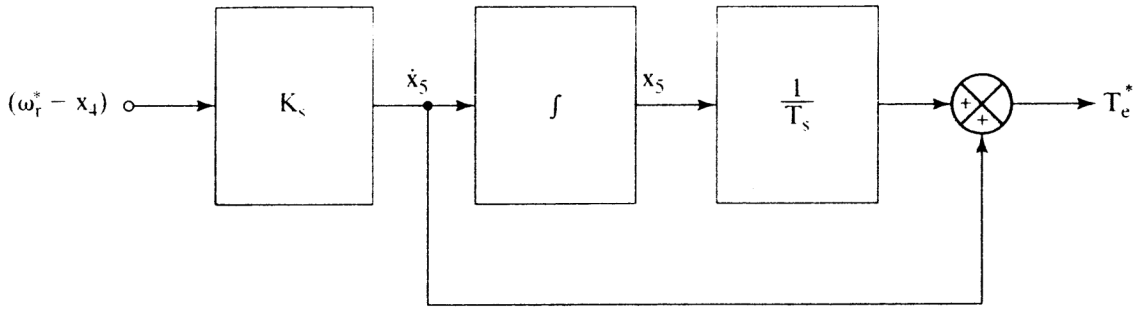

Figure 4.29 State diagram of the speed controller

4.13.3 Speed Controller

The input to the speed controller is the speed error, and the controller is of a PI type given by

$$\frac{T_e^*(s)}{(\omega_r^* - \omega_{mr})} = \frac{K_s(1 + sT_s)}{sT_s} \tag{4.95}$$

The state diagram of the speed controller is shown in Figure 4.29, where

$$y_1 = (\omega_r^* - \omega_{mr}) \tag{4.96}$$

The state equation and the torque equation are

$$\dot{x}_5 = K_s y_1 = K_s(\omega_r^* - \omega_{mr}) = K_s(\omega_r^* - x_4) \tag{4.97}$$

$$T_e^* = \frac{x_5}{T_s} + \dot{x}_5 = \frac{x_5}{T_s} + K_s y_1 = \frac{x_5}{T_s} + K_s(\omega_r^* - x_4) = -K_s x_4 + \frac{1}{T_s}x_5 + K_s\omega_r^* \tag{4.98}$$

There is a limit on the maximum torque command, which is included as a constraint as

$$-T_e(\max) \le T_e^* \le +T_e(\max) \tag{4.99}$$

4.13.4 Command Current Generator

The current command is calculated from the torque command and is given as

$$i_a^* = \frac{T_e^*}{Mi_f} = \frac{T_e^*}{M} \cdot \frac{1}{x_3} \tag{4.100}$$

Substituting for T_e^* from equation (4.98) into (4.100) gives the current command as

$$i_a^* = \left(-\frac{K_s}{M}\right)\cdot\frac{x_4}{x_3} + \left(\frac{1}{T_s M}\right)\cdot\frac{x_5}{x_3} + \frac{K_s}{M}\cdot\frac{\omega_r^*}{x_3} \tag{4.101}$$

4.13.5 Current Controller

The current error is

$$i_{er} = i_a^* - i_a \tag{4.102}$$

which, in terms of the motor and controller parameters, is

$$i_{er} = \left(-\frac{K_s}{M}\right)\cdot\frac{x_4}{x_3} + \left(\frac{1}{T_s M}\right)\cdot\frac{x_5}{x_3} + \left(\frac{K_s}{M}\cdot\omega_r^*\right)\cdot\frac{1}{x_3} - x_1 \tag{4.103}$$

The current-controller logic is illustrated for hysteresis control. It is given as

$$i_{er} > \Delta I, \quad \text{set } V_a = V_s \tag{4.104}$$

$$i_{er} < -\Delta I, \quad \text{reset } V_a = 0 \tag{4.105}$$

Note that the control logic considers only the forward-motoring mode. Suitable logic has to be incorporated for the rest of the quadrants' operation. For PWM control, the logic given by equations (4.61) and (4.62) is used.

4.13.6 System Simulation

The anti-windup controller for the speed controller can be modelled and can be incorporated in place of the PI speed controller. For the example illustrated in the following pages, the anti-windup circuit is not incorporated with the PI speed controller. Equations (4.89), (4.90), (4.91), (4.94), and (4.97) constitute the state equations; equations (4.100), (4.104), and (4.105) are to incorporate the limits and current controller. The solution of the state equations is achieved by numerical integration, with ω_r^* serving as the only input into the block diagram. A flowchart for the dynamic simulation is given in Figure 4.30.

Typical dynamic performance of a speed-controlled chopper-fed dc motor drive is shown in Figure 4.31. The current controller is of hysteresis type, and a 0.25-p.u. steady-state load torque is applied. 0.5 p.u. step speed is commanded, with a maximum torque limit of 2 p.u. resulting in the armature current limit of 2 p.u. The current window is 0.1 p.u., sufficient to cause low switching frequency for this drive system. The references are shown with dotted lines. The torque response is obtained in 1.3 ms, and the speed response is uniform and without any noticeable oscillations. Note that, as the rotor speed reaches the commanded speed, the speed error (and hence the electromagnetic torque command) decreases. During this time, to reduce the electromagnetic torque, only zero voltage is applied across the armature terminals. When the armature current goes below its reference value, then the source voltage is applied to the armature.

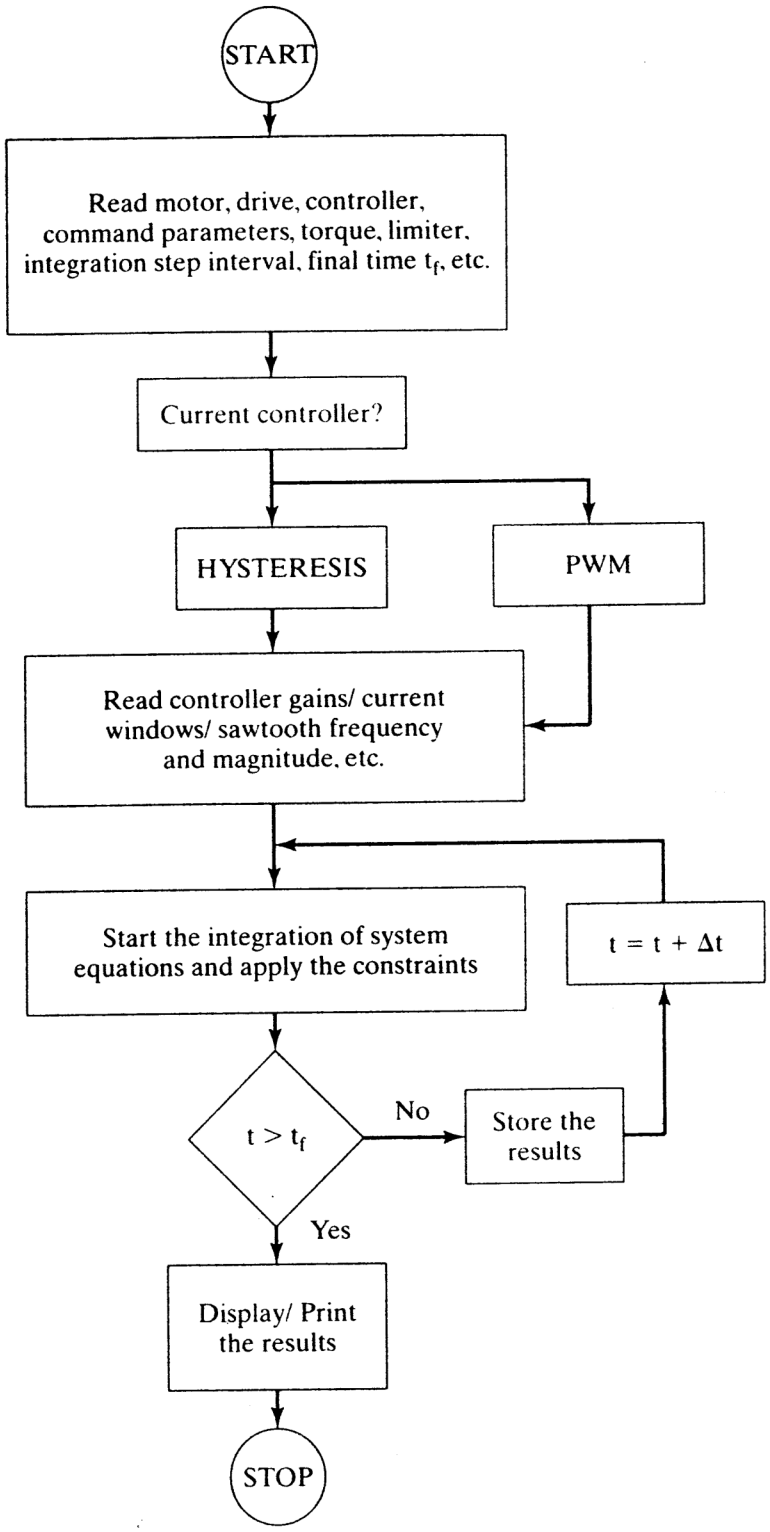

Figure 4.30 Flowchart for the dynamic simulation of the chopper-controlled dc motor drive